

REPORT 1370

AREA-SUCTION BOUNDARY-LAYER CONTROL AS APPLIED TO THE TRAILING-EDGE FLAPS OF A 35° SWEEP-WING AIRPLANE¹

By WOODROW L. COOK, SETH B. ANDERSON, and GEORGE E. COOPER

SUMMARY

A wind-tunnel investigation was made to determine the effects on the aerodynamic characteristics of a 35° swept-wing airplane of applying area-suction boundary-layer control to the trailing-edge flaps. Flight tests of a similar airplane were then conducted to determine the effect of boundary-layer control on the handling qualities and operation of the airplane, particularly during landing.

The wind-tunnel and flight tests indicated that area suction applied to the trailing-edge flaps produced significant increases in flap lift increment. Although the flap boundary-layer control reduced the stall speed only slightly, a reduction in minimum comfortable approach speed of about 12 knots was obtained.

INTRODUCTION

Reference 1 indicated that much less air flow and power were required to obtain boundary-layer control at a wing leading edge with suction through a porous area than through a slot. It was therefore reasoned that similar gains in suction requirements would be realized if boundary-layer control were applied by suction through a porous surface near the forward edge of trailing-edge flaps.

Because of the possibility of the power requirements with area suction being low enough to be of practical value, an investigation was conducted on the 35° sweptback wing F-86 airplane in flight and in the Ames 40- by 80-foot wind tunnel. Area suction was applied at several trailing-edge flap deflections through various chordwise extents and positions of porous surface. It was anticipated that maximum lift would be limited by leading-edge air-flow separation on the wing; thus, the investigations also included the use of the suction flap with (1) a modified wing leading having camber and increased leading-edge radius, and (2) a wing leading-edge slat.

In the flight tests, the landing approach with and without boundary-layer control was evaluated by 16 Air Force, Navy, contractor, and NACA pilots. The results of these evaluations are examined in this report to determine the relationship between the pilots' opinions of the several configurations flown and their choice of minimum comfortable landing-approach speed.

NOTATION

A_x	longitudinal acceleration
A_n	normal acceleration
BLC	boundary-layer control
b	wing span, ft
c	chord, measured parallel to the plane of symmetry, ft
\bar{c}	mean aerodynamic chord, $\frac{2}{S} \int_0^{b/2} c^2 dy$, ft
C_D	drag coefficient, $\frac{\text{drag}}{qS}$
C_L	lift coefficient, $\frac{\text{lift}}{qS}$
$C_{L_{max}}$	Maximum lift coefficient
C. L. E.	cambered leading edge
C_m	pitching-moment coefficient computed about the quarter-chord point of the mean aerodynamic chord, $\frac{\text{pitching moment}}{qS\bar{c}}$
C_q	flow coefficient, $\frac{Q}{\sqrt{S}}$
d	chordwise extent of porous surface, measured in chord plane, ft
F_G	gross thrust
F_R	ram drag
I. A. S.	pilots' indicated airspeed as read from cockpit indicator, knots
$\frac{L}{D}$	lift-to-drag ratio
l	length of porous surface, measured along surface normal to leading edge, in.
p_∞	free-stream static pressure, lb/sq ft
p	static pressure, lb/sq ft
P	airfoil pressure coefficient, $\frac{p_i - p_\infty}{q}$
P_d	average duct pressure coefficient, $\frac{p_d - p_\infty}{q}$
P_p	plenum-chamber pressure coefficient, $\frac{p_p - p_\infty}{q}$
q	free-stream dynamic pressure, lb/sq ft

¹ Summarizes NACA Research Memorandums A53E06 by Woodrow L. Cook, Curt H. Holzhauser and Mark W. Kelly, A55K14 by George E. Cooper and Robert C. Innlis, and A55K29 by Seth B. Anderson and Hervey C. Quigley.

Q	volume of air removed through porous surface, cu ft/sec, based on free-stream density at test attitude
R	Reynolds number, $\frac{V\bar{c}}{\nu}$
S	wing area, sq ft
t	thickness of porous material, in.
V	free-stream velocity, ft/sec
V_A	calibrated approach airspeed, knots
$V_{C_{L,max}}$	calibrated airspeed corresponding to maximum lift coefficient, knots
w	suction-air velocity, ft/sec
W	assumed weight of airplane, $C_L q S$
$\left(\frac{W}{S}\right)_A$	wing loading for approach condition (1000 lb of fuel remaining)
x	chordwise distance, parallel to plane of symmetry, ft
y	spanwise distance, perpendicular to plane of symmetry, ft
z	height above wing reference plane, ft
α	angle of attack of fuselage center line, deg
δ_f	flap deflection, measured in plane normal to the hinge line, deg
$\hat{\delta}_f$	flap deflection, measured in plane parallel to plane of symmetry (δ in ref. 2), deg
Δp	pressure drop across porous material, lb/sq ft
Λ	sweep angle, deg
ν	kinematic viscosity, ft ² /sec

SUBSCRIPTS

crit	critical
d	duct
f	trailing-edge flap
L	leading edge
p	plenum chamber
R	reference conditions
l	local surface

MODEL AND APPARATUS

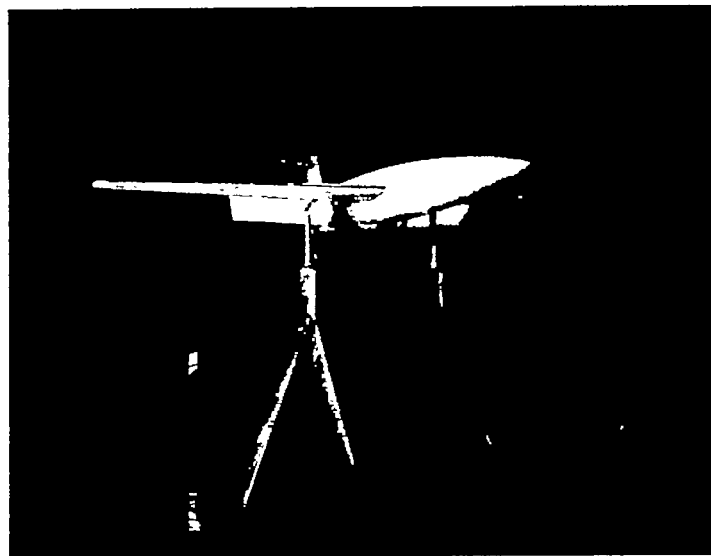
WIND-TUNNEL MODEL

A general view of the model is shown in figure 1 (a). Except for the flaps, the model is the same as that used in the investigation of reference 1 where it is described completely. The geometric characteristics of the model are shown in figures 2 (a) and 3. Additional dimensions of the model are provided in table I. The wing panels and horizontal tail are from an F-86A airplane. The horizontal tail is in the same position relative to the wing as on the airplane. The coordinates for the airfoil section at two spanwise sections are given in table II.

The original trailing-edge flaps on the wing were removed and replaced with suction flaps that could be deflected to 45°, 55°, 64°, and 70°. The flaps has a constant chord and extended from 0.135 to 0.495 semispan. The flap chord of the wind-tunnel model was larger than that on the flight airplane, as is shown in figure 4. The flaps were constructed with the upper surface porous over the axis of rotation (fig. 4). The porous surface extended from a point $\frac{1}{2}$ inch aft of the reference line to 8 inches aft of the reference line measured along the surface normal to the reference line. The reference

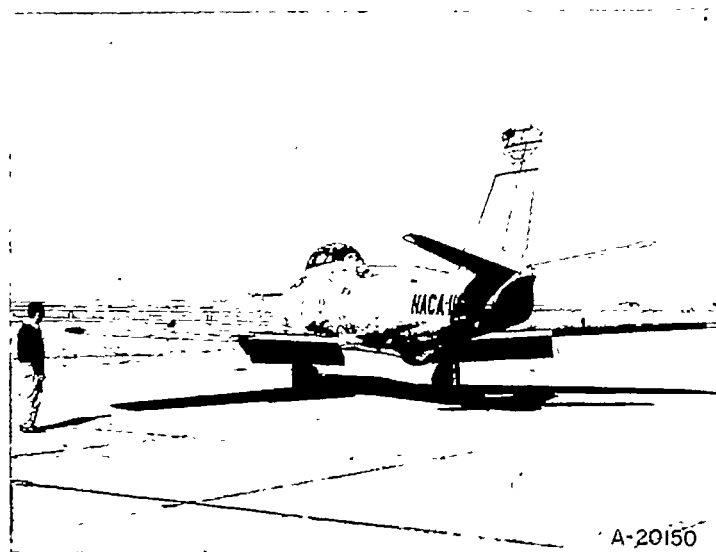
line shown in figure 4 is a line on the upper surface of the wing in a vertical plane with the hinge line. The chordwise extent and position of porous surface was controlled with a non-porous tape of about 0.003-inch thickness. The various extents and positions of porous areas tested are listed in table III. The dimensions given are normal to the reference line and are measured along the curved porous surface. The chordwise extent of the porous surface for all configurations was constant across the span of the flap.

The porous material used for the flap was the same type used in the investigation of reference 1. The material was composed of a metal mesh sheet backed with a white wool felt material. The metal mesh sheet had 4,225 holes per square inch, and was 11 percent open and 0.008 inch thick. The flow resistance characteristics for the porous material are shown in figure 5 for two grades of wool felt, each having $\frac{1}{8}$ -inch thickness. For other thicknesses of felt, the pressure



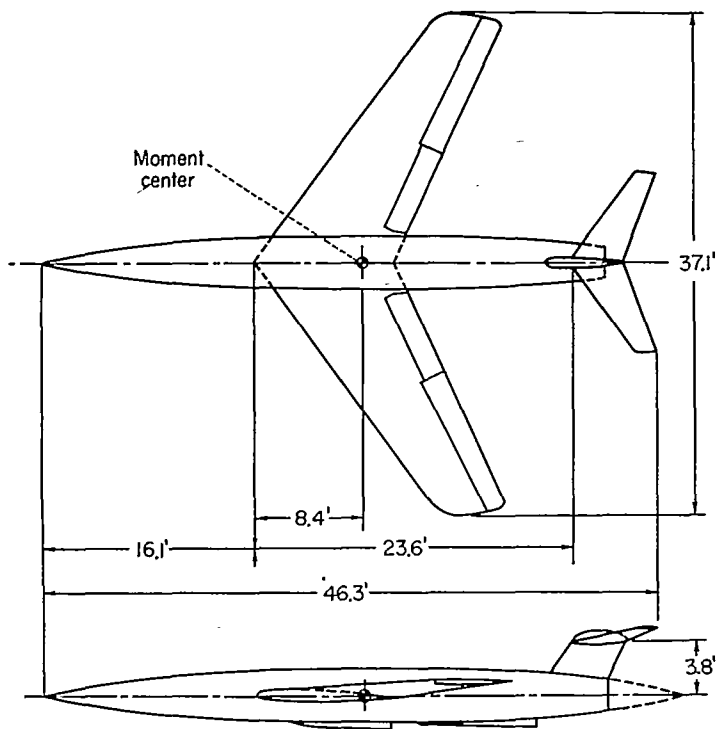
(a) The 35° sweptback wing wind-tunnel model.

FIGURE 1.—General arrangements of the test vehicles equipped with area suction flaps.

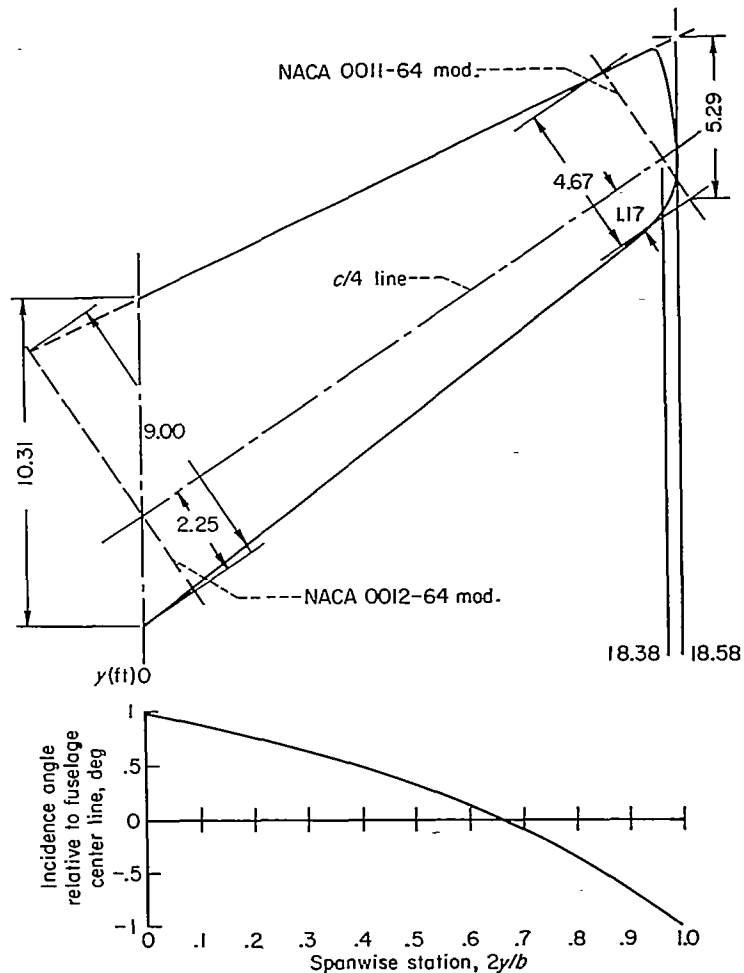


(b) The F86-A airplane.

FIGURE 1.—Concluded.

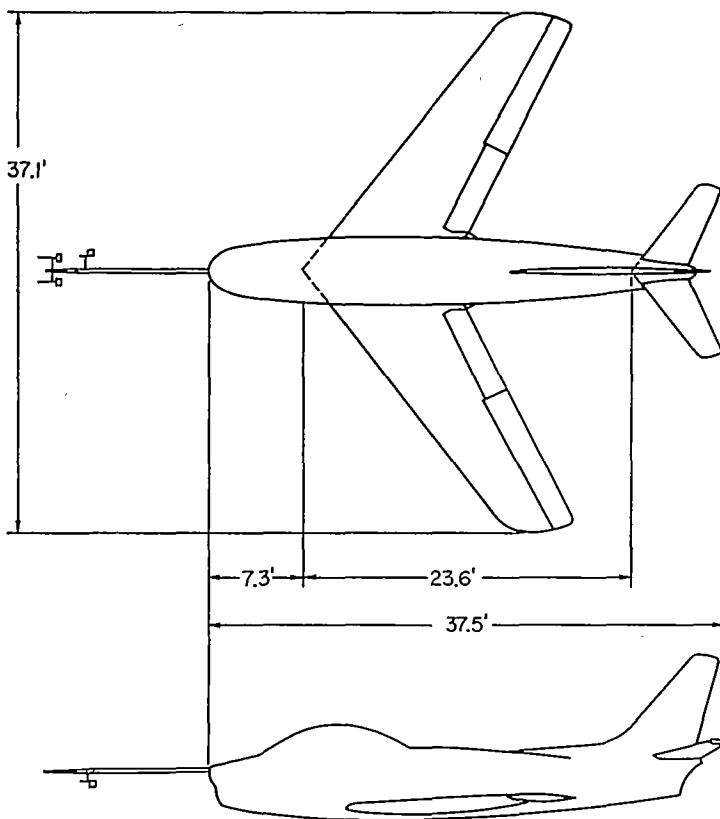


(a) 35° swept wing wind-tunnel model.
 FIGURE 2.—Geometry of test vehicles.



Note: Coordinates of airfoil given in table II.
 Sweep angle of quarter-chord line in plane of wing 34°58'
 All dimensions in feet

FIGURE 3.—Wing geometry.



(b) Flight-test airplane.
 FIGURE 2.—Concluded.

drop across the surface was directly proportional to thickness of the wool felt. The variation of thickness of a tapered felt is also shown in figure 5. Because of the external pressure variation over the flap, variations in thickness are used to give a more uniform chordwise distribution of suction-air velocity, as discussed in reference 1.

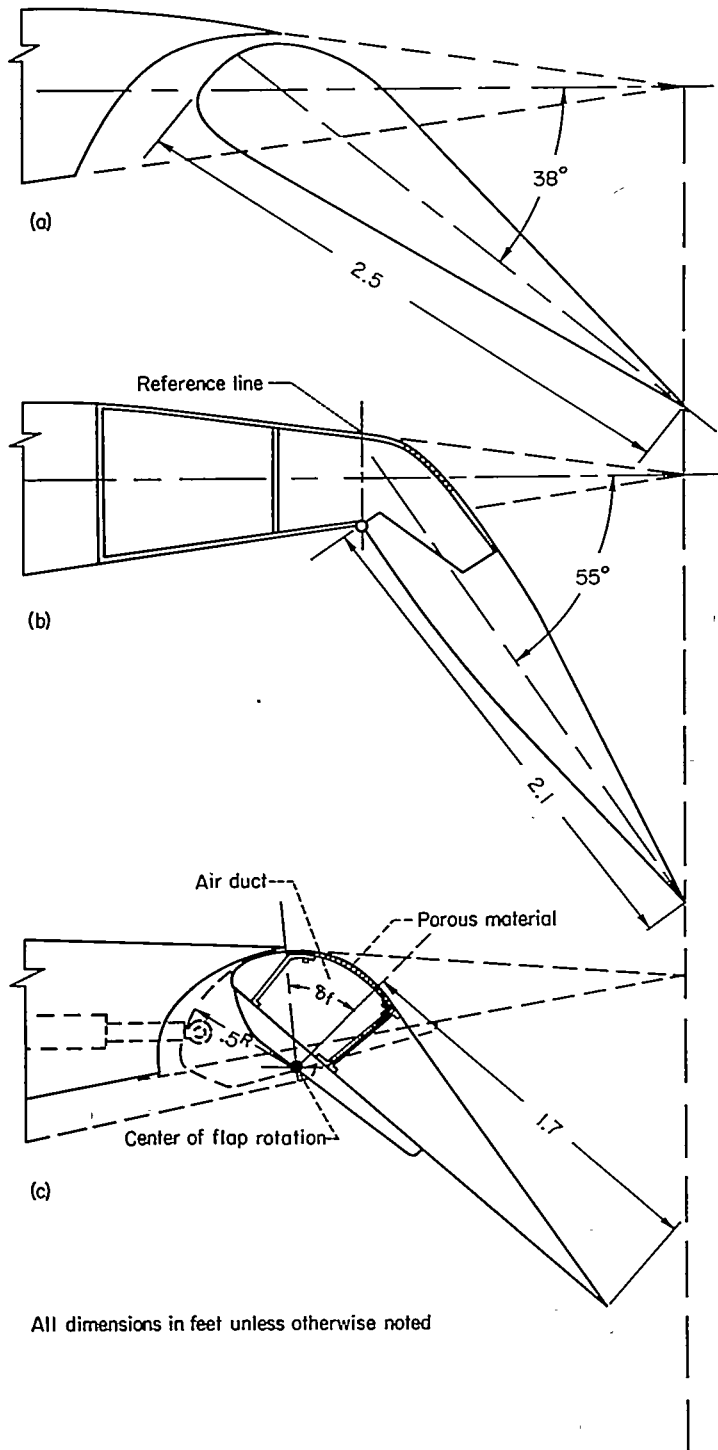
The model was tested with three wing leading-edge configurations. The majority of the tests were made with the normal F-86A leading edge for which the coordinates are given in table II. Two leading edges were used to enable studies of the area-suction flap at higher lift coefficients: (1) the modified leading edge which had camber added to the forward portion of the chord, and an increased leading-edge radius as shown in figure 6 (a) and table IV and (2) the F-86A leading-edge slat, shown in figure 6 (b), extending from 0.245 semispan to 0.94 semispan.

The fuselage used in the wind-tunnel tests was circular in cross section, and the radius, in feet, is defined by the equation

$$1.84 \left[1 - \left(\frac{x}{23} - 1 \right)^2 \right]^{3/4}$$

This fuselage has a larger fineness ratio (11.5) and smaller width ($0.10 b/2$) than the fuselage of the F-86 airplane (fineness ratio 6.9, and $0.13 b/2$ width). With this fuselage the wing was mounted at a mid-fuselage position in contrast to the low wing position of the F-86 airplane.

The suction system consisted of a centrifugal compressor driven by an electric motor mounted in a plenum chamber in the fuselage. The air was drawn through the wing surface,

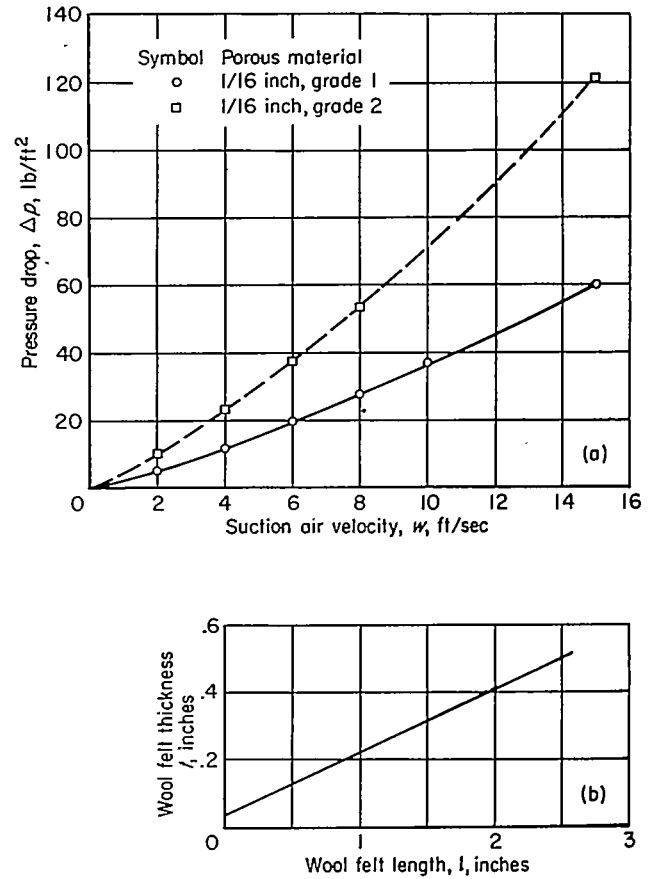


All dimensions in feet unless otherwise noted

(a) Slotted flap.
 (b) Area-suction flap, wind-tunnel model.
 (c) Area-suction flap, airplane.

FIGURE 4.—Cross sections of various trailing-edge flaps.

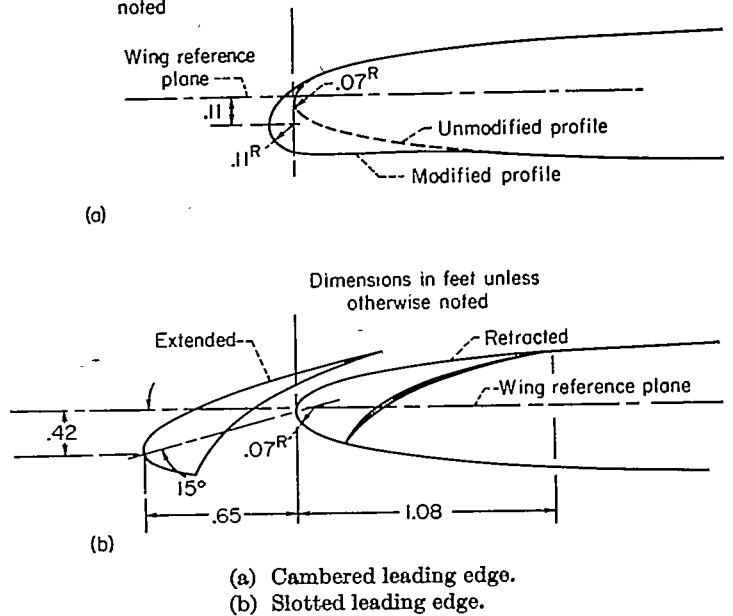
into wing ducts, through the plenum chamber and the compressor, and out the exit duct at the bottom of the fuselage. The quantity of air removed was measured by survey rakes located at the exit of the system. The rakes were calibrated



(a) Flow characteristics.
 (b) Chordwise distribution. Grade 1 felt.

FIGURE 5.—Chordwise distribution of porous surface and flow characteristics of two grades of porous material.

Dimensions in feet unless otherwise noted



(a) Cambered leading edge.
 (b) Slotted leading edge.

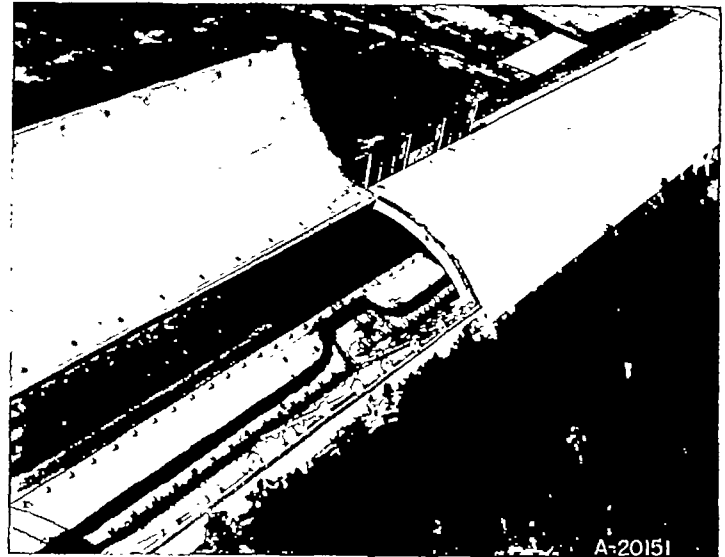
FIGURE 6.—Cross sections of the various leading edges.

with standard ASME orifice meters. Plenum-chamber and duct pressures were measured with static-pressure orifices and were assumed to be equal to the total pressure, since the suction-air velocities in the duct and plenum chamber were low. The spanwise and chordwise positions of surface-pressure orifices are listed in table V. The total suction power was measured with a wattmeter and included pump losses, duct losses, and the suction requirements.

FLIGHT-TEST AIRPLANE

The installation of the area-suction flap was made on an F-86A-5 airplane. Figure 1 is a photograph showing the airplane with the boundary-layer-control equipment installed. The test airplane dimensions are presented in table I and a two-view drawing is shown in figure 2. Some of the boundary-layer-control equipment was mounted externally to facilitate installation. The external modifications to the airplane consisted of a faired pod, enclosing an ejector pump for supplying suction, and ducts on the underside of the fuselage for removing air from the flaps (see fig 7). Air was bled from the last stage of the compressor of the J-47 engine through a pilot-controlled butterfly valve to the primary nozzle of the ejector pump. The weight of the boundary-layer-control equipment for this research-type installation was 105 pounds. Considerable savings in weight should be possible in a production-type installation.

The F-86A slotted flap was modified to a plain type by reworking the nose section, removing the flap tracks, and mounting external hinge brackets on the under surface of the wing. This mounting allowed flap deflections up to 65°. The portion of the flap ahead of the flap spar was used as a duct and is shown in figure 7. A sketch of the flap cross section is given in figure 4 (c). Boundary-layer air was drawn in through a graded porous material of sintered stainless steel, which had the permeability characteristics shown in figure 8. It should be noted that the characteristics shown in figure 8 were not measured but were those specified to the manufacturer and were designed for a uniform inflow velocity of 3.75 feet per second (at $\delta_p=55^\circ$) on the basis of pressure-



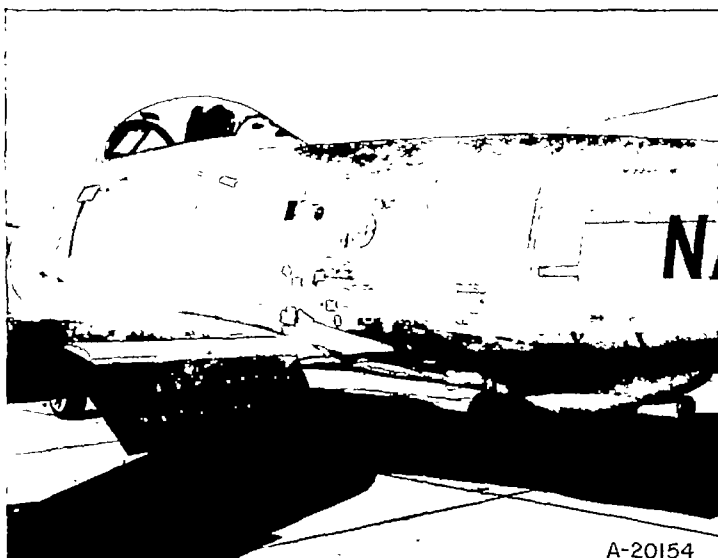
(b) Internal duct and porous material.

FIGURE 7.—Concluded.

distribution data obtained from the 40- by 80-foot wind-tunnel tests. The chordwise length and placement on the flap of the porous material were estimated also from the wind-tunnel tests. The porous material was formed easily, was readily adapted to the flap structure, and had a reported tensile strength of approximately 15,000 pounds per square inch.

The airplane was fitted with modified leading edges which replaced the slats for some of the flights. The modified leading edge consisted of a cambered leading edge having an increased radius similar to the leading edge used in the wind-tunnel tests. With this leading edge, tests were conducted both with and without a 0.20c wrap-around fence (0.05c height) at 63-percent spanwise section.

Standard NACA instruments were used to record airspeed, altitude, acceleration, duct pressures, and angle of attack. Values of airspeed and angle of attack were measured



(a) External flap duct and ejection pump.

FIGURE 7.—Close-up view showing area suction flap on airplane.

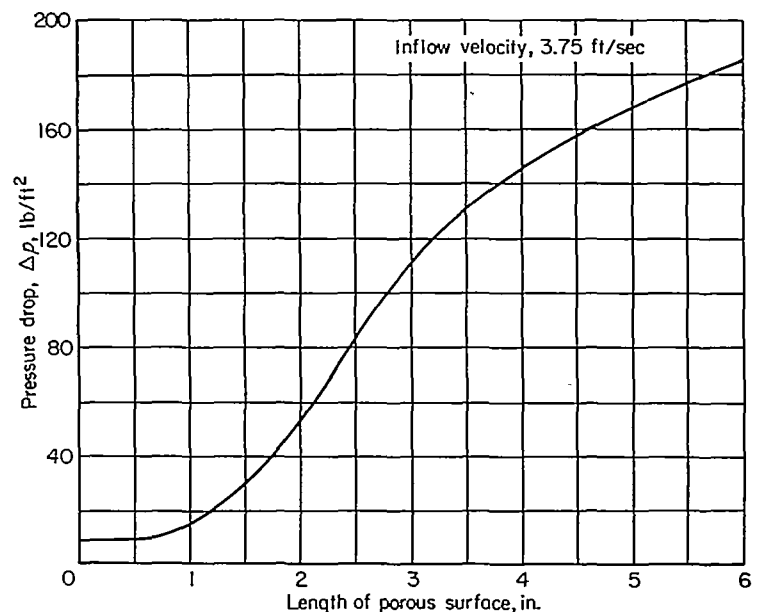


FIGURE 8.—Variation of pressure drop with chordwise length of porous surface for flight test airplane.

approximately 8 feet ahead of the fuselage nose. Duct pressures in the flap were measured at the midspan station of the flap. The flow quantity drawn through the porous material was measured by calibrated rakes in the ducts. Measurements taken on the ground with a flowmeter indicated uniform inflow velocities along the span of the flap.

TESTS AND CORRECTIONS

WIND TUNNEL

The primary purpose of the investigation was to determine the relation between the lift increments realized from the flap and the suction power and flow quantities required. Three-component force data were obtained at zero sideslip for all flap and wing configurations. For some conditions, pressure distributions over the wing were obtained. In addition, tests were made with the horizontal tail removed to show the effects on longitudinal stability.

Initial tests showed that as suction was increased, the lift increment first increased rapidly, then quite abruptly the rate of increase fell off to a very low value. The test procedure, therefore, was to determine for each model arrangement and angle of attack the power and suction quantities required to reach the point where further increases in these quantities gave little increase in lift increment. The values of flow coefficient and lift coefficient at this point are called $C_{q_{crit}}$ and $C_{L_{crit}}$, respectively. In the tests the angle of attack and free-stream velocity were held constant and the suction quantity was varied.

For the model with the unmodified wing leading-edge profile, an extensive investigation was made for 45°, 55°, 64°, and 70° of flap deflections of the effect of position and extent of the porous area. Table III presents a summary of the porous area arrangements tested. Data were obtained at Reynolds numbers of 7.5×10^6 and 9.6×10^6 . For the model with wing leading-edge modifications, only one flap deflection, 55°, and only one arrangement of porous area (config. 1) on the flap were tested.

The standard tunnel-wall corrections for a straight wing of the same area and span as the sweptback wing were applied to the angle of attack, pitching-moment, and drag-coefficient data. This procedure was followed since an analysis indicated that tunnel-wall corrections were approximately the same for straight and swept wings of the size under consideration. The following increments were added:

$$\begin{aligned}\Delta\alpha &= 0.61 C_L \\ \Delta C_D &= 0.0107 C_L^2 \\ \Delta C_m &= 0.008 C_L \text{ (tail-on data only)}\end{aligned}$$

No corrections were made for strut interference. All flow coefficients were corrected to standard sea-level conditions. The effect of the thrust of the exhaust jets was found to be negligible.

FLIGHT

To obtain the lift and drag characteristics, tests were conducted at altitudes of 10,000 and 2,000 feet over a speed range of 150 knots to the stall. The tests were conducted at an average wing loading of 45 pounds per square foot except as noted, with the center of gravity at 22.5-percent

mean aerodynamic chord. The engine rpm was held fixed for a given series of test runs. For the data presented in this report, an engine rpm of 70 percent was used (approximate rpm used in landing approach). In obtaining the data for the lift curves presented herein, no attempt was made to change the amount of bleed air to the primary nozzle of the ejector pump with airspeed so as to maintain a critical value of C_q .

The initial phase of the landing-approach evaluation was flown by a total of 16 Air Force, Navy, contractor, and NACA pilots. For comparison purposes, most of the pilots also flew a standard F-86A-1 equipped with 38° flaps and 10° leading-edge slats. (For the major portion of the data reported herein, the normal (15°) F-86A-5 type slats were used on the wing leading edge.) Each pilot was requested to furnish the following information on each different configuration flown: stall speed, stall characteristics, and opinion of stall, the minimum comfortable approach speed at landing weight,² and the primary reasons for choosing that particular approach speed. The Navy and NACA pilots made their evaluation based on the requirements for a carrier approach and landing. The Air Force pilots, in general, made 360° overhead, partial power, sinking-type approaches, which started at approximately 1,000-foot altitude over the touchdown point. While the carrier-type approach may be defined by a single approach speed, it was noted that with the sinking approach at least three different speeds at different points in the pattern were considered necessary by most pilots to define adequately any given approach. For reasons of simplicity and comparison in those cases where three speeds were given, only the over-the-fence speed has been used as it was found to be more similar to the carrier-approach speed.

Another phase of the investigation comprised field carrier-landing evaluation flights of the suction-flap airplane with several leading-edge combinations. This phase of the evaluation was conducted by four NACA research pilots.

In the calculation of the measured stalling speeds and thrust-required curves, the value of wing loading used for each airplane was that corresponding to 1000 pounds of fuel remaining. This is given below for each test airplane.

Standard airplane.....	42.3 lb/sq ft
Suction-flap airplane.....	42.6 lb/sq ft

The value of gross weight for which many of the pilots reported stalling speeds was not accurately known. This factor undoubtedly contributed to the scatter in the reported stalling speeds, as well as to the differences between reported stalling speeds and the measured values based on $C_{L_{max}}$. For the standard airplane, this discrepancy is further aggravated by an unreliable but large error in indicated airspeed below about 102 knots. Consequently, the measured rather than reported value of stall speed has been used for all comparative purposes.

The airspeed covering the approach speed ranges was calibrated in flight for the airplanes. This made possible correlation between pilot-reported speeds of the airplanes, as well as between these speeds and the various measured

² Landing weight as used herein is defined as the gross weight with 1000 pounds of fuel remaining.

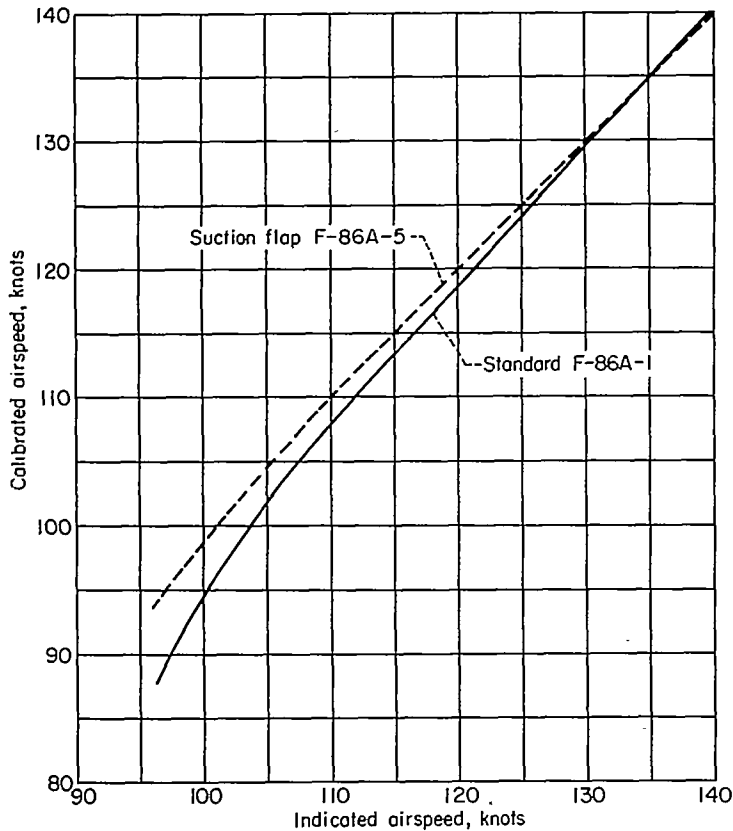


FIGURE 9.—Flight determined airspeed calibration curves.

quantities. With the exception of table VI, which gives pilot-reported stall and approach speeds in terms of the

pilot's indicated airspeed, all other airspeed values are calibrated speeds and were obtained from pilots' indicated speeds using the flight-determined calibration curves of figure 9.

The equations used to determine the lift coefficients and drag coefficients are as follows:

$$C_L = \frac{W}{qS} (A_x \cos \alpha + A_z \sin \alpha) - \frac{1}{qS} (F_G \sin \alpha)$$

$$C_D = \frac{W}{qS} (A_x \sin \alpha - A_z \cos \alpha) + \frac{1}{qS} (F_G \cos \alpha - F_R)$$

In the equations above, the first portion is for the accelerations on the airplane, while the second portion is for the thrust force acting on the airplane. The gross thrust and engine air flow were determined from measurements of the total pressure and temperature in the tail pipe of the jet engine.

Measured stalling speeds were determined using the measured values of $C_{L_{max}}$ with a correction for thrust based on the thrust required at the approach airspeed.

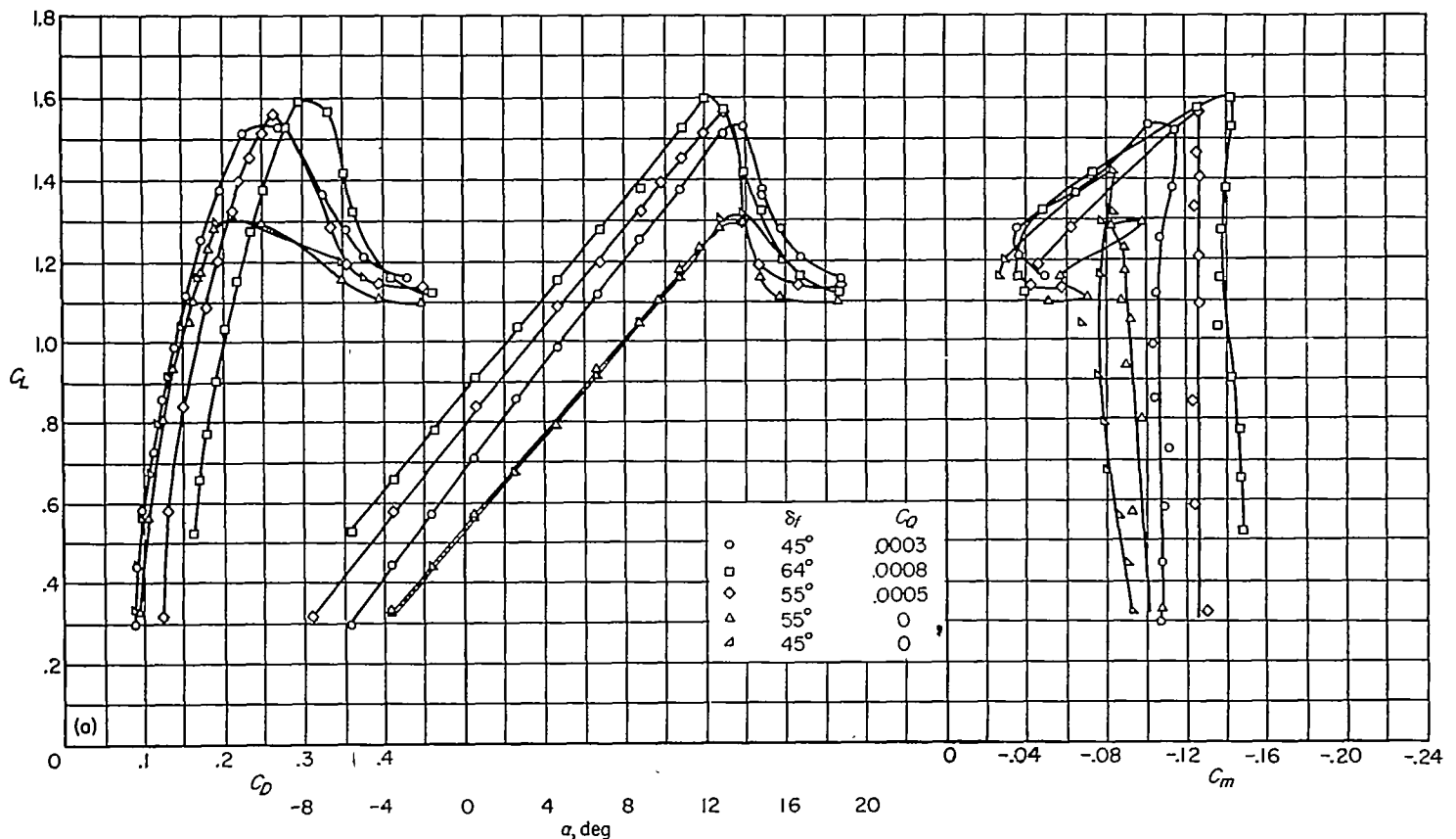
Thrust-required curves were determined at landing weight for each configuration by the following relationship:

$$\text{Net thrust from the engine required for level flight} = \frac{\text{drag}}{\cos \alpha}$$

RESULTS AND DISCUSSION

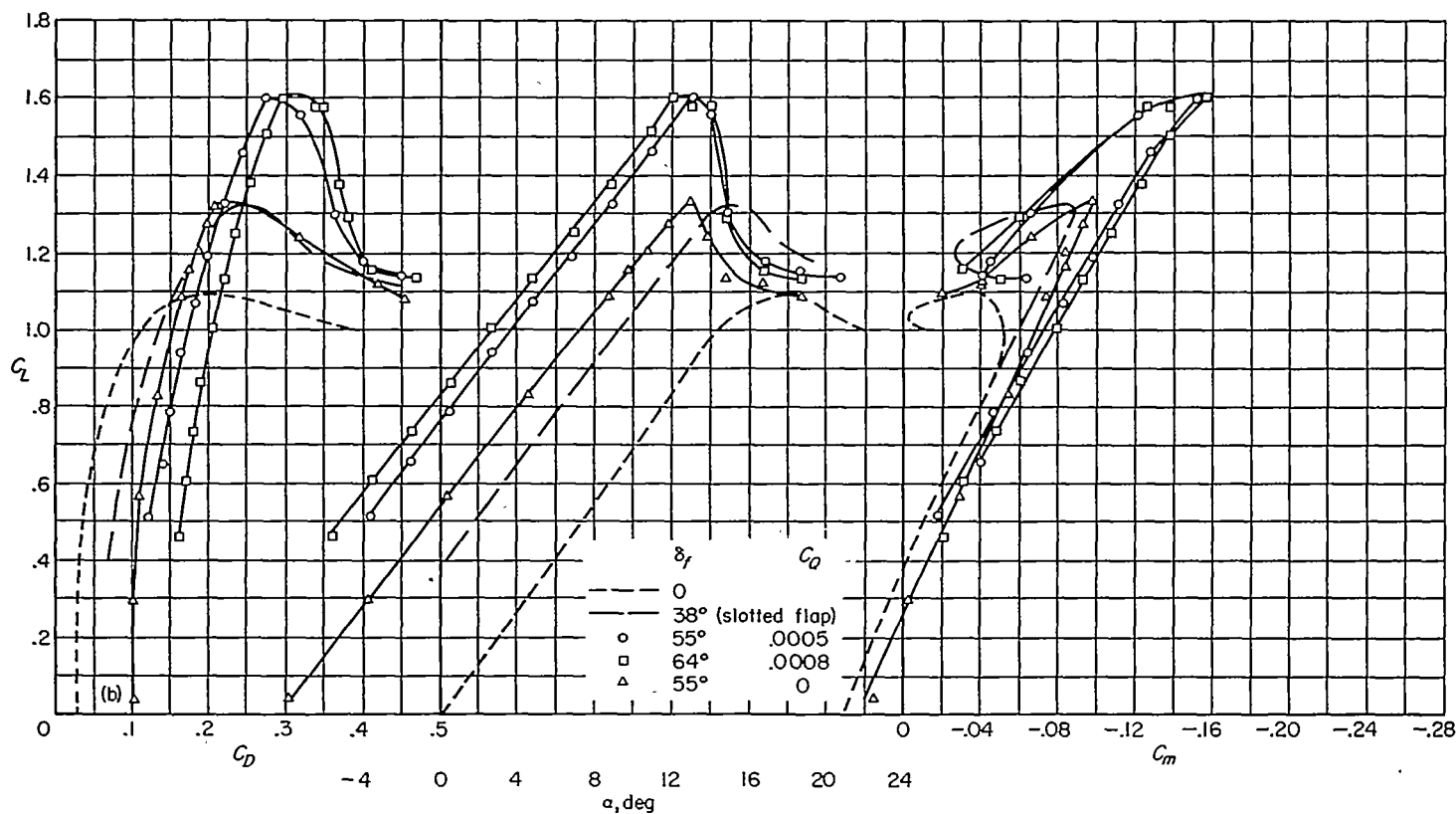
WIND-TUNNEL TESTS

Static-longitudinal characteristics with area suction applied to trailing-edge flaps.—The lift, drag, and pitching-moment data are shown in figure 10 with the trailing-edge flaps de-



(a) Horizontal tail off.

FIGURE 10.—Aerodynamic characteristics of the 35° swept wing model with area-suction trailing-edge flaps; plain leading edge.



(b) Horizontal tail on.

FIGURE 10.—Concluded.

flected 45°, 55°, and 64°. The results are shown with and without suction on the flap and are compared with the slotted flap deflected 38°. The results indicate that an appreciable increase in flap lift increment, ΔC_L , can be obtained up to 64° flap deflection with area suction applied throughout the angle-of-attack range up to the angle for maximum lift coefficient. Representative pressure distributions are shown in figure 11.

The flap lift increments obtained with suction applied at an angle of attack of 0° are compared in figure 12 to theoretical values³ calculated by the method of reference 2. On this wing with area suction applied to the trailing-edge flaps, flap effectiveness above 90 percent of theoretical values is obtained to 64° of flap deflection. Although the theory is limited in its accuracy when wing-fuselage effects are considered, it is also known that some air-flow separation did exist on the trailing-edge flaps at all deflections, as indicated by tuft studies and by the pressure distribution shown in figure 11; and therefore higher flap lift increments possibly even greater than the theoretical values would be expected with more complete elimination of air-flow separation on the flaps. The use of 70° flap deflection with suction gave no more flap lift increment than the 64° flap deflection.

The gain in flap lift increment with area suction applied was retained at nearly a constant value to maximum lift

coefficient with the normal wing leading edge. The maximum lift coefficient was established by leading-edge air-flow separation occurring on the wing from approximately mid-semispan to the tip, as indicated by the pressure distributions shown in figure 11, as well as by observations of the tufts on the wing. In order to study the effect of area suction on the flap at higher lift coefficients, tests were made with a modified wing leading edge and a wing leading-edge slat, both used to delay the occurrence of leading-edge air-flow separation. The effect of the leading-edge devices on the lift, drag, and pitching-moment characteristics is shown by a comparison of figures 13 and 10 (b). With the modified leading edge and flap deflection of 55°, the flap lift increment with area suction was almost constant to maximum lift; $C_{L_{max}}$ was 1.97, whereas with the normal leading edge it was 1.61. However, with the partial-span leading-edge slat, a reduction in flap lift increment occurred at about an angle of attack of 6° which was traced to rough air flow from the discontinuity, formed by the inboard end of the slat and the wing leading edge, causing air-flow separation to occur on the flap over an area directly aft of the discontinuity. With the slats, a value of $C_{L_{max}}$ of 1.7 was obtained. From these results, it is concluded that the major effect of applying area suction to trailing-edge flaps is to increase lift at a given attitude.

Suppression of air-flow separation on the flaps caused no particular change in pitching moment, with horizontal tail on, except to extend the linear range of pitching moment to higher lift coefficients. In the tail-off case, the increase in flap lift increment was accompanied by an increase in pitching moment. With area suction applied, the pitching

³ The theoretical flap effectiveness was computed from reference 2.

$$\Delta C_L = \left(\frac{d\alpha}{d\delta_f} \right) C_{L\delta_f} \frac{\delta_f}{57.3} \quad (\text{equivalent to eq. (7), ref. 2})$$

for the subject wing
 $C_{L\delta_f} = 1.52$ (cross plot of fig. 5, ref. 2)
 $d\alpha/d\delta_f = 0.61$ (curve of theoretical flap effectiveness, fig. 3, ref 2; $c_l/c = 0.26$, average value perpendicular to flap hinge line)
 $\tan \delta_f = \cos \Lambda / \tan \delta_f = 0.895 \tan \delta_f$
 $\Delta C_L = \frac{(0.61)(1.52)}{57.3} \delta_f = 0.0162 \delta_f$

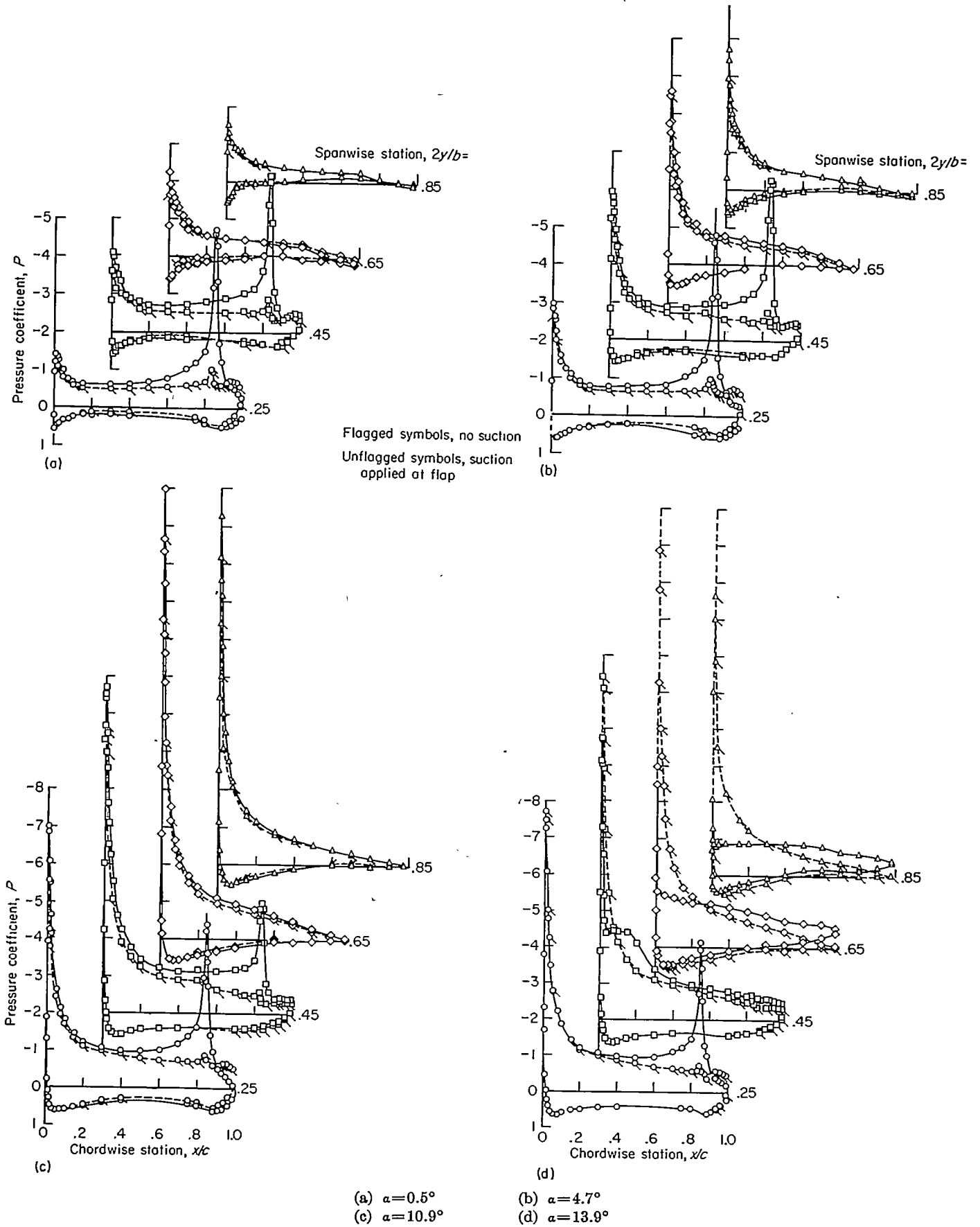


FIGURE 11.—Effect of area suction on the chordwise pressure distributions; $\delta_f = 55^\circ$.

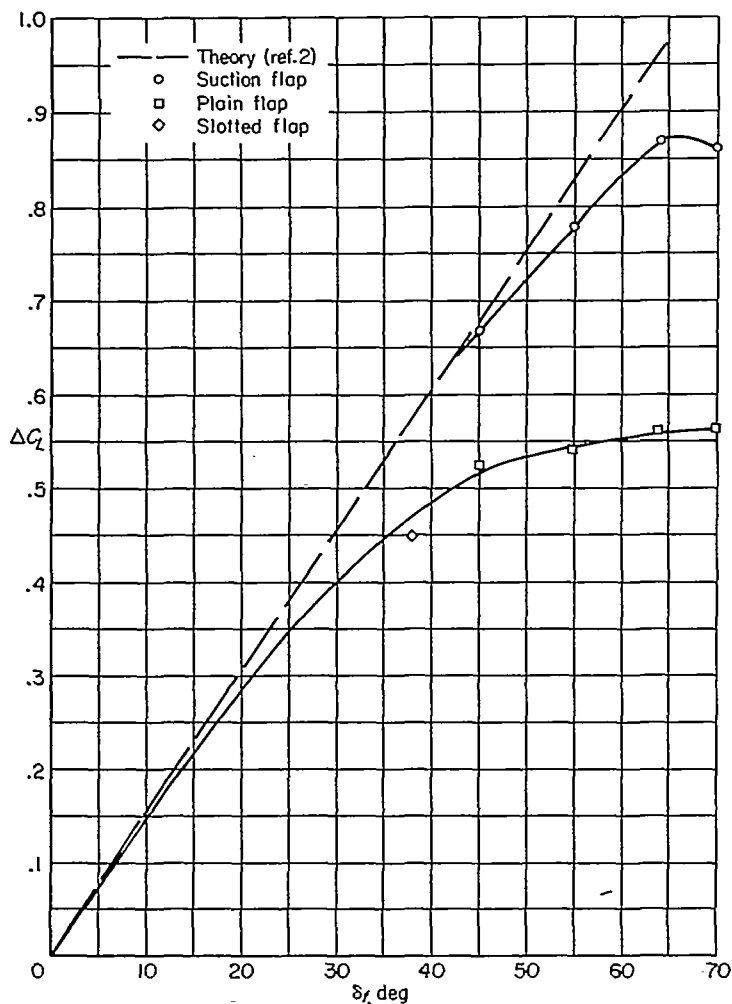


FIGURE 12.—Variation of flap lift increment with flap-deflection angle.

moment per unit of flap lift increment at a given angle of attack is 0.155, compared to a value of 0.185 for plain flap without suction. Presumably, this results from a forward movement of center of pressure at a given angle of attack as air-flow separation is suppressed on the flap. The increase in pitching moment with boundary-layer-control application may be of greater importance for larger flap lift increments, for example, with greater spanwise extent of flaps than studied herein the maximum lift of the horizontal tail would be approached for trimmed conditions.

With boundary-layer control applied to the flaps, the data in figure 10 indicate an increase in drag at a given lift coefficient or angle of attack. The increase in drag is due to the particular spanwise extent of flap which, with the application of suction, results in a span loading considerably more distorted from the ideal elliptical loading than the span loading obtained without boundary-layer control. It is deduced that the increase in induced drag due to the distorted loading is considerably greater than the reduction in profile drag due to suppression of air-flow separation and hence there is an over-all increase in drag. A decrease in drag with boundary-layer control would be expected with flaps of larger span.

Suction requirements of area-suction flap.—Figure 14 shows the variation of flap lift increment with flow coefficient

for four flap deflections. These data were obtained at an angle of attack near 0° and for one location and chordwise extent of porous area. Similar data were obtained at other angles of attack and other configurations of porous area. Examination of all these data showed the following facts which are generally applicable to each flap deflection:

1. For any configuration of porous area, as flow coefficient was increased, an initial slow rise in lift was followed by an abrupt rise to a particular value which could be increased only slightly by further large increases in flow coefficient.

2. For any one configuration of porous area, the variation of lift increment with flow coefficient was essentially the same at all angles of attack, provided the angle of attack was less than that at which separation of flow appeared at the wing leading edge.

3. For nearly all configurations of porous area, nearly the same total increase in lift occurred as the flow coefficient was increased, but the abruptness of the rise and the flow coefficient at which it occurred were modified by the chordwise extent and location of the porous area.

For each flap deflection, a particular value of lift increment was obtained that was exceeded only slightly with large increases in flow coefficient; for example, with the 55° flap deflection (fig. 14), the ΔC_L increased from about 0.78 to 0.79 with a fourfold increase in flow coefficient from 0.0005 to 0.0020. These values of flap increment are also shown in figure 12, where a comparison is made between the measured values of lift increment for several flap deflection angles and values calculated by the method of reference 2.

The variation of flow coefficient required for a range of flap deflections is shown in figure 15 for three chordwise distributions of suction-air velocities. The required suction-air velocities can be controlled by two methods: first, by having porous surfaces of constant thickness with different pressure-drop characteristics and second, by having a porous surface with chordwise variation of pressure-drop characteristics, as described in reference 1. The pressure-drop characteristics of the materials used in these tests are shown in figure 5. The chordwise distributions of suction-air velocity for the three porous surfaces required to obtain equal values of $\Delta C_{L_{crit}}$ are shown in figure 16 for the flap deflection of 55° . For the least dense porous material (curve (a) of fig. 16), a pumping pressure coefficient of -4.5 was required for boundary-layer control, and the total air-flow coefficient was 0.00049. For a porous surface having twice the pressure drop (curve (b)), the pumping pressure coefficient was -4.9 , and the total flow coefficient was 0.00036, about a 27-percent reduction in air flow. A further reduction in flow coefficient was obtained by using a tapered porous material which represented a porous surface with the pressure drop varying chordwise. The change in thickness of the porous material, shown in figure 5(b), varied as the external surface pressure with the thinnest or low-pressure-drop section at the forward edge near the peak negative pressure and the thick or high-pressure-drop section at the aft edge where the external surface pressure was less negative. With this tapered porous surface, the chordwise distribution of suction-air velocities required to prevent air-flow separation is shown by curve (c) in figure 16.

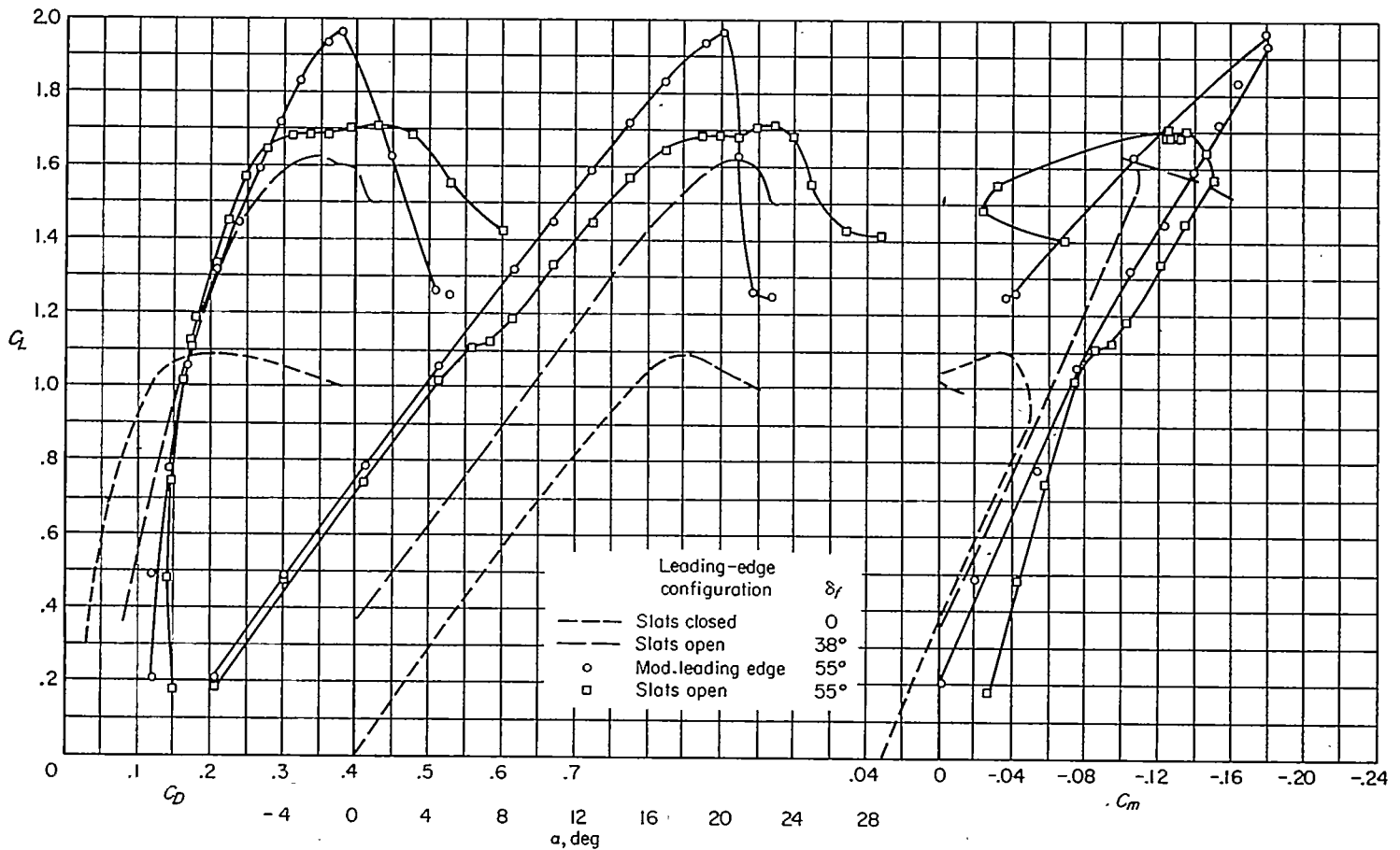


FIGURE 13.—Aerodynamic characteristics of the 35° swept-wing model with area-suction flaps and two wing leading-edge devices; horizontal tail on; $C_q=0.0005$ for $\delta_f=55^\circ$.

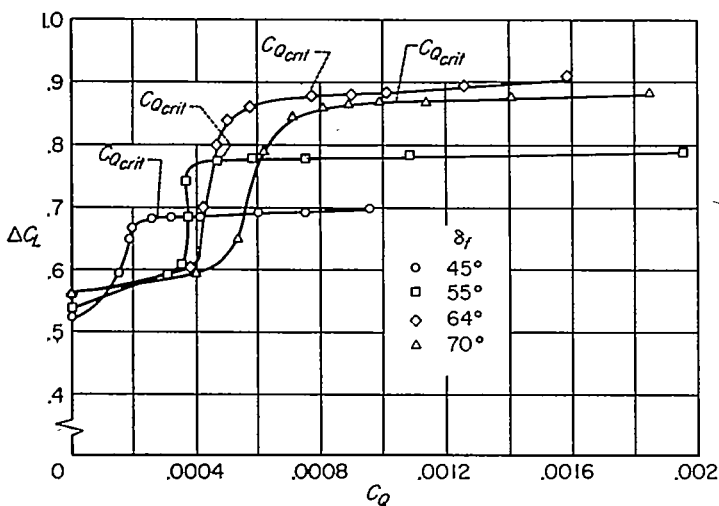


FIGURE 14.—Variation of flap lift coefficient increment with suction flow coefficient; $R=7.5 \times 10^6$.

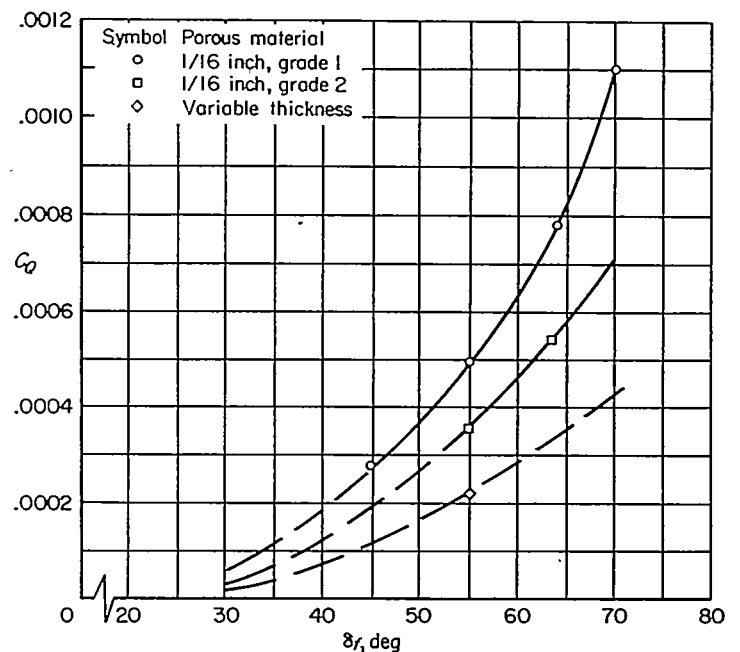


FIGURE 15.—Variation of flow-coefficient requirements with flap-deflection angle for three types of porous materials; $R=9.6 \times 10^6$.

A pumping pressure coefficient of -5.3 was required to obtain this distribution, resulting in a flow coefficient of 0.00022 or a 55-percent reduction of total flow from the first case of the constant thickness high-porosity material. It can be concluded that the proper distribution of suction-air velocities is required to obtain low flow coefficients.

A limited study was made of the effect of Reynolds number and angle of attack or wing lift coefficient on the flow coefficients required for boundary-layer control.

These results shown in figure 17 indicate that within the range studied, there is essentially no effect of either Reynolds number or wing lift coefficient on the flow coefficients required for area-suction-type boundary-layer control. There is, however, a significant effect of angle of attack or

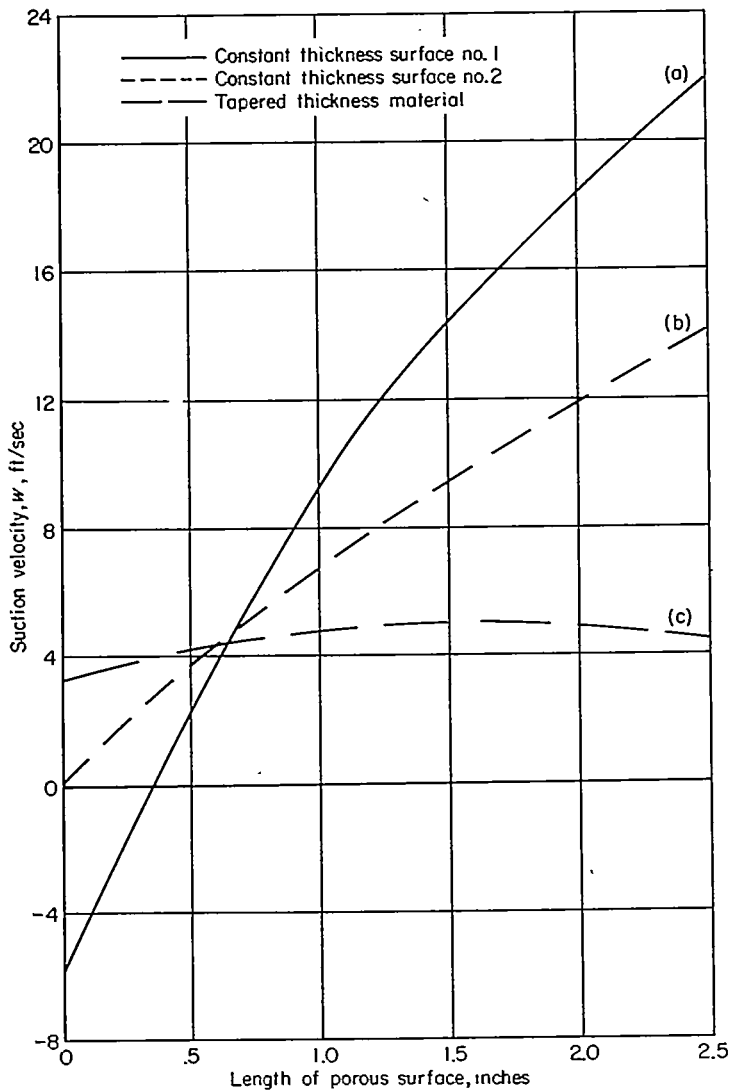


FIGURE 16.—Chordwise distribution of suction-air velocities for three types of porous material; $\delta_f = 55^\circ$, $R = 9.6 \times 10^6$.

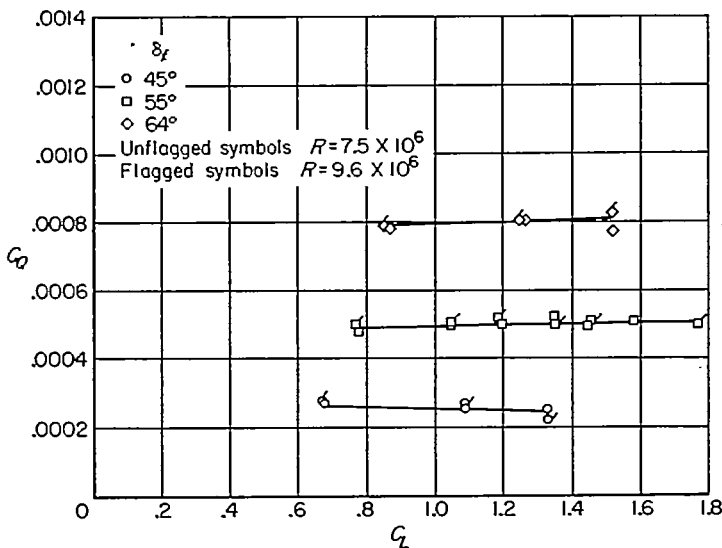


FIGURE 17.—Effect of wing lift coefficient and Reynolds number on flow-coefficient requirements.

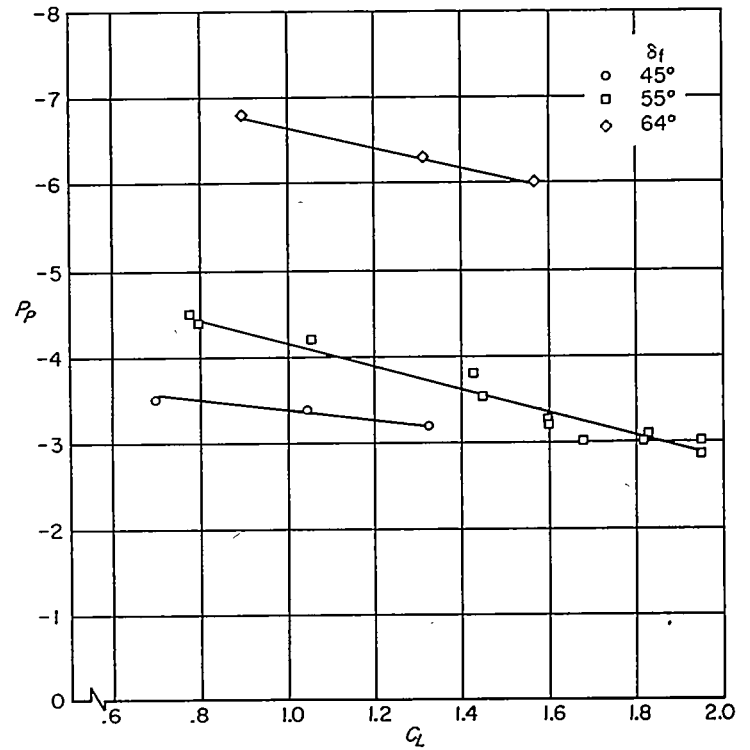
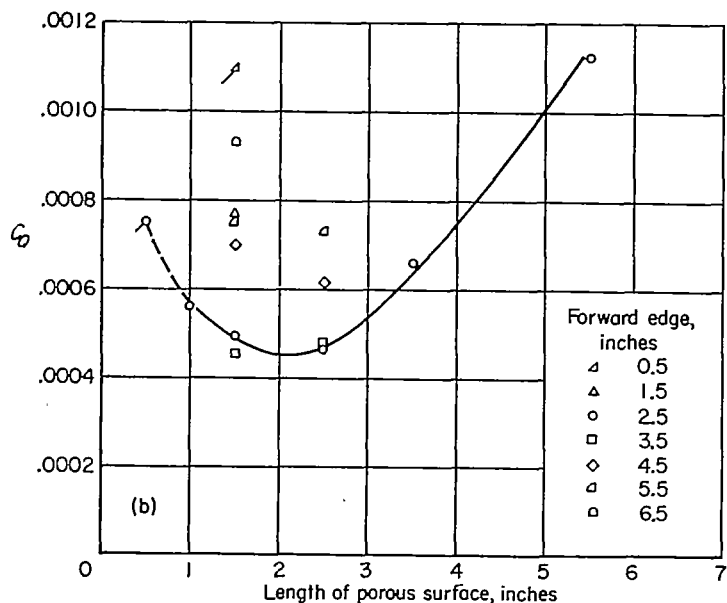
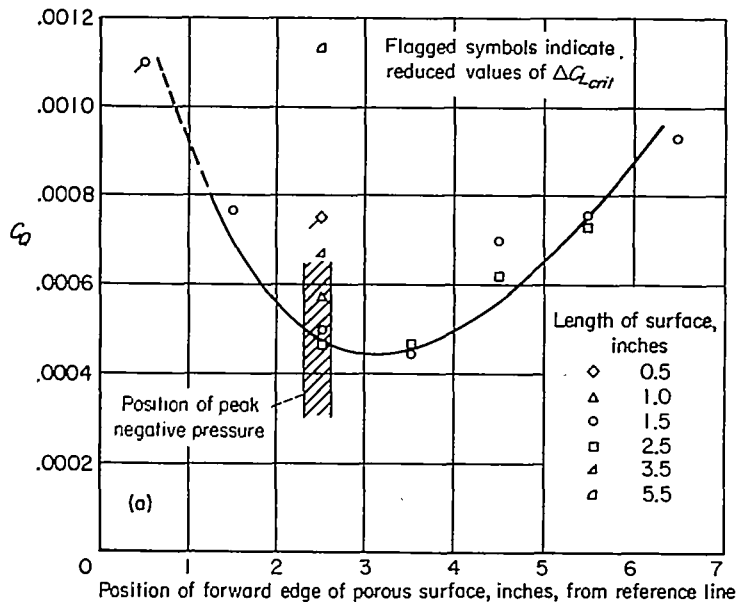


FIGURE 18.—Variation of plenum-chamber pressure coefficient with wing lift coefficient.

wing lift coefficient on the suction pressure coefficient (fig. 18). This effect, decreasing magnitude of pressure coefficient with increasing angle of attack, was due entirely to a reduction in magnitude of peak negative pressure coefficient over the porous surface with wing angle of attack. Such a drop in peak pressure is not compatible with potential theory. It was concluded that air-flow separation was not completely eliminated on the flaps and that more air-flow separation existed at the higher angles of attack. As in the case of flow coefficient, the suction pressure coefficient was independent of free-stream velocity.

It was noted previously that the value of $\Delta C_{L_{crit}}$ could be obtained with numerous variations of porous surface position and extent. It was also noted that to obtain $\Delta C_{L_{crit}}$, the value of $C_{Q_{crit}}$ varied for each configuration of porous area. Figures 19, 20, and 21 have been prepared to show the variation of $C_{Q_{crit}}$ for several configurations of porous area for 55° , 64° , and 70° of flap deflection. The effects of two variables are shown in each figure, first, the effect of position of several extents of porous area, and second, the effect of the extent of porous opening with the forward edge at a fixed point.

The results shown in figures 19 (a), 20 (a), and 21 (a) indicate that there is a particular position for the forward edge of the porous opening which results in minimum $C_{Q_{crit}}$, and that this position is not greatly affected by the extent of opening—at least within the range tested. Figures 18 (b), 19 (b), and 20 (b) indicate that with the forward edge at the position for minimum $C_{Q_{crit}}$, for any of the extents, there is also a particular extent required to realize minimum $C_{Q_{crit}}$. These results were obtained with the

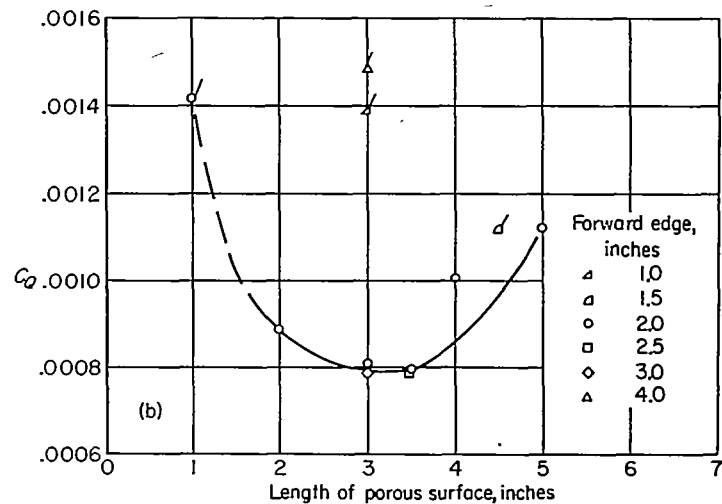
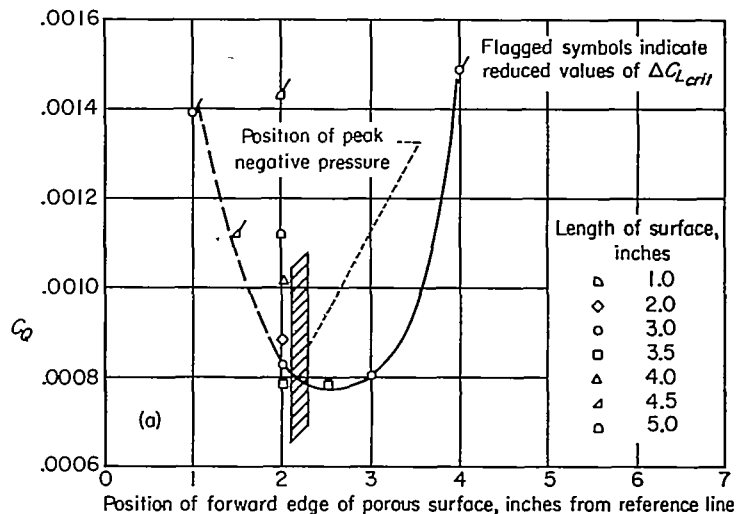


(a) Porous-surface position.
(b) Porous-surface extent.

FIGURE 19.—Variation of flow coefficient required for $\delta_f=55^\circ$ with extent and position of porous area; $\Delta C_{L_{crit}}=0.78$, $R=7.5 \times 10^5$.

low-pressure-drop porous surface, grade number 1, but the results shown indicating the chordwise location and extent of porous surface for minimum flow coefficient are typical of those for the other two porous surfaces studied. While the foregoing results serve to show trends, it would appear reasonable to assume they are not quantitatively applicable to other wing-flap arrangements.

It has been shown previously (ref. 1), in connection with application of area suction to control separation of air flow from the leading edge of a wing, that area suction is most effective when the forward edge of the porous area coincides with the point of maximum negative pressure. That this is also true in the case of the flap is indicated by the relative positions of the maximum negative pressure measured over the flap and the position of the forward edge of the porous



(a) Porous-surface position.
(b) Porous-surface extent.

FIGURE 20.—Variation of flow coefficient required for $\delta_f=64^\circ$ with extent and position of porous area; $\Delta C_{L_{crit}}=0.87$, $R=7.5 \times 10^5$.

area for minimum flow-coefficient requirement. Suction forward of this point results in needlessly withdrawing air in the region of a favorable pressure gradient. Moving the leading edge of the area suction progressively aft resulted in not only increased flow requirements but, as found during this investigation, instability of the flow and, finally, inability to attain the value of $\Delta C_{L_{crit}}$ obtained with the best positions and extents of porous area. It thus appears that the optimum location for the forward edge of the porous area will, for any plain flap, be at or very close to the point of maximum negative pressure.

General conclusions with regard to the extent of the porous area are not so readily reached. It can be conjectured from the results shown in figures 19, 20, and 21 that the position of the aft edge of the porous area for the minimum flow coefficient is at the point where the boundary layer is just sufficiently stable to withstand the subsequent pressure recovery without aid. If the porous area is not carried to this optimum point, then the boundary layer must be made

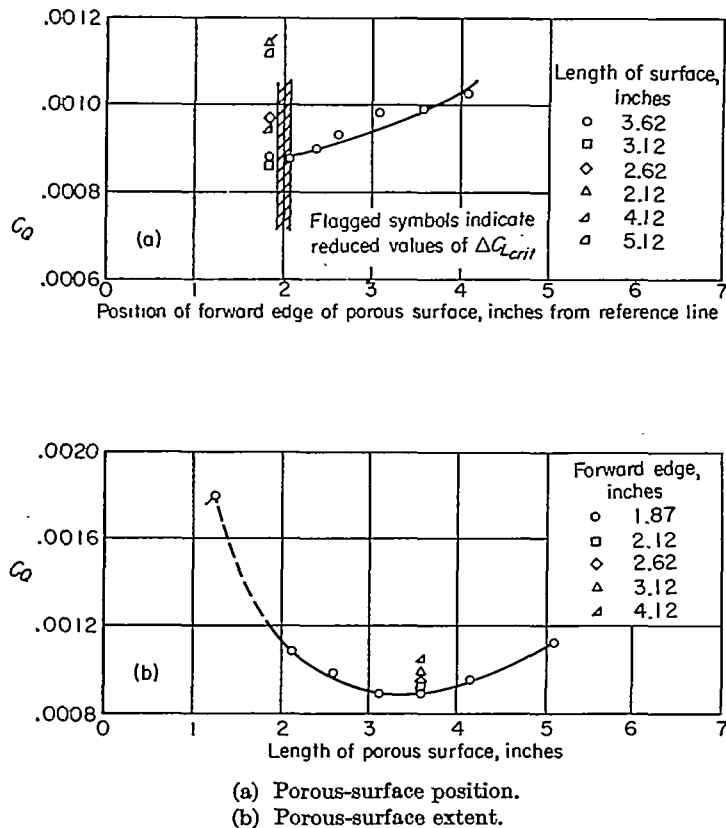


FIGURE 21.—Variation of flow coefficient required for $\delta_f = 70^\circ$ with extent and position of porous area; $\Delta C_{L_{crit}} = 0.86$, $R = 7.5 \times 10^5$.

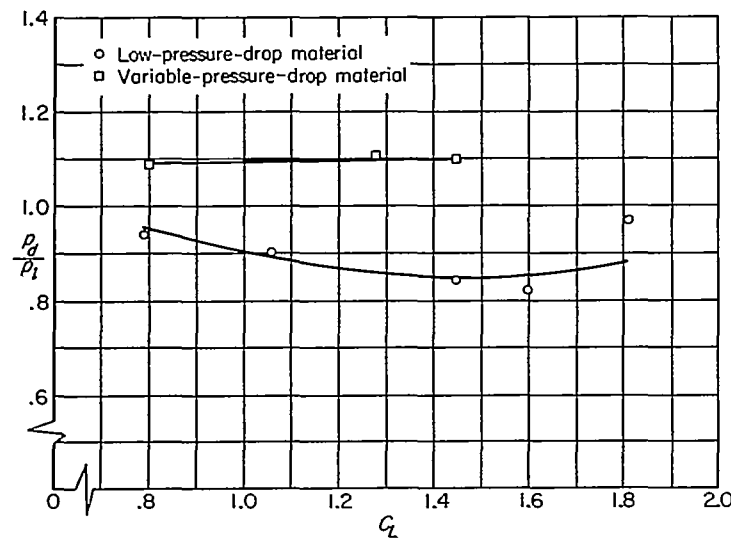


FIGURE 22.—Variation of suction pressure ratio (duct pressure to flap peak pressure) with wing lift coefficient for two types of porous surface.

more stable than in the case just mentioned; that is, larger flow coefficients would be required to suppress flow separation beyond the region of porous area. If the porous area is carried beyond the optimum point, air would be withdrawn needlessly. As yet, however, no method analogous to that shown in reference 1 is available for predicting the required extent of porous area in the case of the flap.

The total suction power required is a function of plenum-chamber pressure coefficient, as well as flow coefficient.

The plenum-chamber coefficient P_P must have a sufficiently negative value to overcome duct losses, pressure drop through the porous material at the required flow rate, and the external negative pressure. In the present investigation, the duct losses and pressure drop through the material were negligible compared to the negative pressure peak over the flap; hence, the required values of P_P are almost entirely a result of the external surface pressure, especially for the least-dense constant-thickness porous material. The variations with lift coefficient of the ratio of plenum-chamber pressure to external surface pressure are shown in figure 22. A surprising feature for the low-pressure-drop constant-thickness material is that the ratio is less than 1.0 for a large part of the lift-coefficient range. For all the points shown, the forward edge of the porous area was at the location for minimum $C_{D_{crit}}$; as noted previously, this location is near the peak negative pressure, indicating that some outflow of air occurred near the forward edge (curve (a), fig. 16). Such an occurrence does not seem favorable to any form of boundary-layer control, and it is probable that the outflow in these cases was possible only because excess air was being withdrawn through a major portion of the porous area (curve (a), fig. 16). With the airflow distribution controlled by chordwise porosity variation (curve (c), fig. 16), the value of the ratio of plenum-chamber pressure to peak negative pressure was significantly greater than 1.0, as shown in figure 22, which indicates that for near the minimum values of flow coefficient of the suction air, the required internal duct pressures will have to be somewhat greater than the peak negative pressures.

The actual power requirements for an airplane are specified in terms of wing loading and landing or take-off speeds. In order to determine these values without the uncertainties of estimating flow coefficient and pressure coefficient, wind-tunnel data were obtained and suction powers measured at conditions corresponding to level flight at wing loadings of 40 and 60 pounds per square foot for 55° and 64° flap deflection with the low-pressure-drop porous surface and at a wing loading of 40 pounds per square foot for 55° of flap deflection with the variable-pressure-drop porous surface. For 64° flap deflection, the measured powers were also obtained with the high-pressure-drop constant-thickness material at a wing loading of 40 pounds per square foot. The measured values of suction horsepower required to obtain $\Delta C_{L_{crit}}$ and the corresponding flow coefficients and plenum-chamber pressure coefficients are given in table VII. The measured suction horsepower shown in the table are the power required to drive the pump, as well as duct losses, system leakage, and the effect of pump efficiency. For most conditions, the duct losses and system leakage were very small and caused little increase in power. For all conditions, the pump efficiency ranged between 63 and 67 percent. The results obtained indicate that for this type of airplane, 10 to 25 horsepower would be required for landing approach and take-off, and that at the lower value of power required it is necessary to control the distribution of the suction-air velocities.

It is apparent that more horsepower is required to reach $\Delta C_{L_{crit}}$ at higher forward speeds. This does not appear to

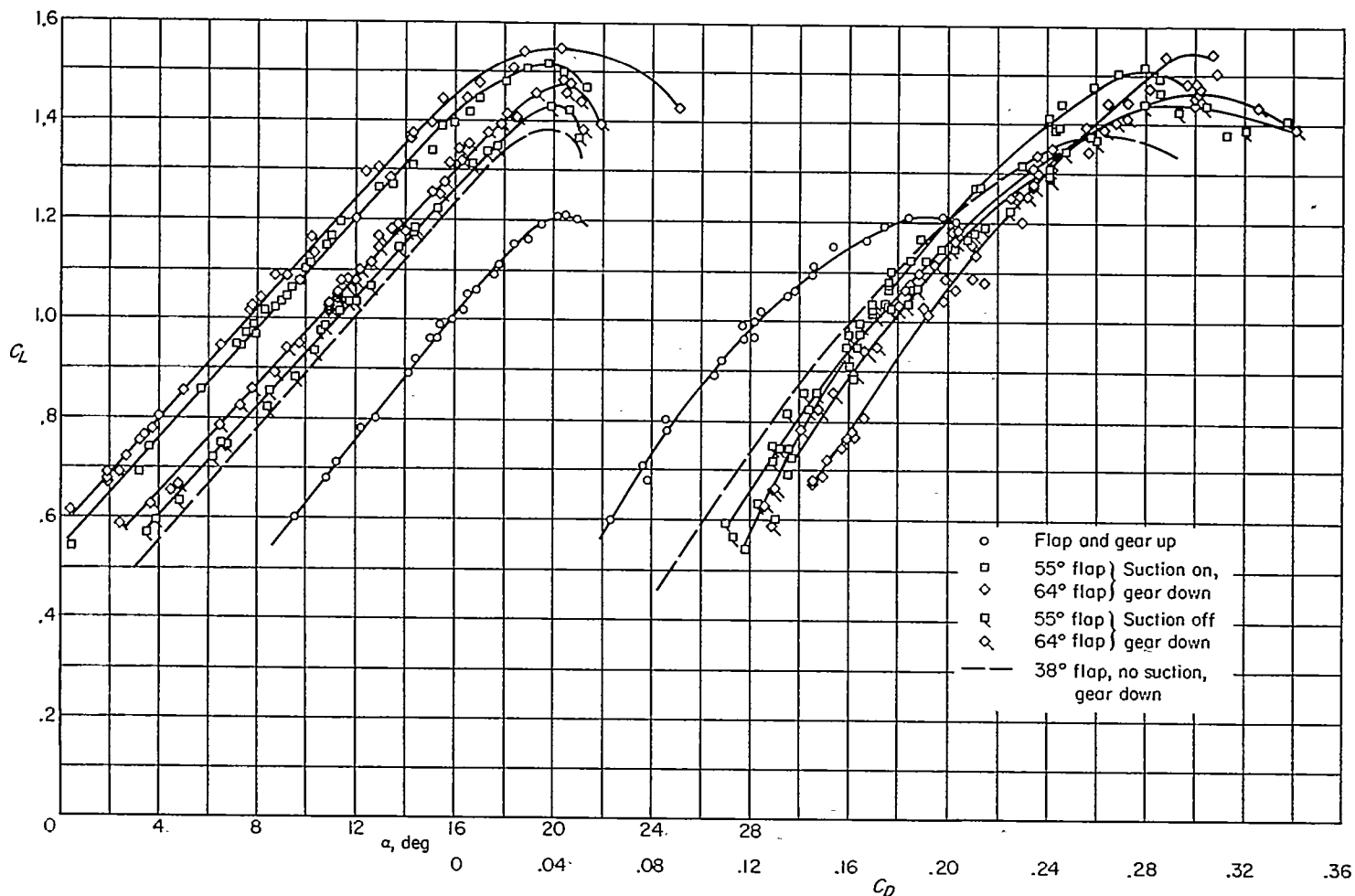


FIGURE 23.—Flight test lift and drag curves, area-suction flaps, and slatted leading edge.

be of particular importance, however, because it was demonstrated during the tests that area suction will cause reattachment of flow when applied where separation exists. Therefore, it would be necessary to supply only the power required to prevent separation at low landing approach speed; as this speed is approached from some higher speed, the flow will attach to the flap.

FLIGHT TESTS

Lift and drag characteristics of airplane with area-suction flaps.—The lift and drag data are presented in figure 23 for flap deflections of 55° and 64° for the flap, and gear-down configuration with boundary-layer control on and off. For comparative purposes, data for the 38° plain flap⁴ with no suction are also shown in figure 23. The data in figure 23 indicate an increase in $C_{L_{max}}$ from 1.38 for the 38° flap to 1.54 for the 64° flap with suction. A comparison of the lift increment of the 64° flap deflection (suction on) with the 38° flap at a constant angle of attack of 11° (average angle of attack used in landing approach) indicates an approximate increase in C_L of 0.24. The lift increment due to suction flaps was essentially constant over the angle-of-attack range except near $C_{L_{max}}$ where there was a 50-percent reduction.

⁴ The plain flap at a deflection of 38° was used as a basis for assessing the effectiveness of the suction flap since, at this deflection, the flap lift increment and lift curves were similar to that obtained with the normal 33° slotted flap on the unmodified airplane (ref. 3). The lift curves from reference 3 were not used directly since drag data, used for performance computation reported herein, were not available from reference 3.

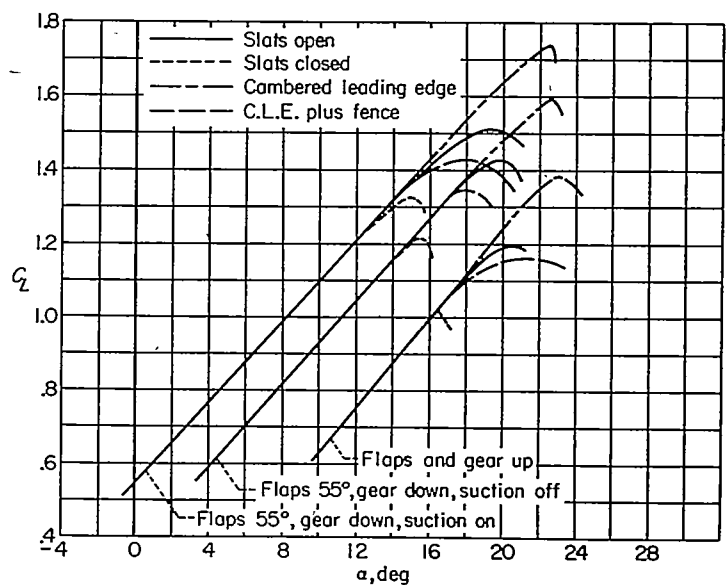


FIGURE 24.—Flight-test lift curves with various leading-edge configurations.

No marked loss in suction lift increment occurred at $\alpha=6^\circ$ as in the tunnel tests. In the tunnel, this loss in lift was felt to be due to a vortex emanating from the inboard end of the slat flowing over the flap and causing an area of separated flow over a portion of the flap. In the flight tests, the duct structure at the wing-fuselage juncture caused flow separation

on the inboard end of the flap and the addition of the vortex flow from the inboard edge of the slat did not increase the amount of separated area at 6° angle of attack as it did in the tunnel.

The lift characteristics of the airplane equipped with various leading-edge devices are summarized in figure 24 for a flap deflection of 55° . These data indicate that the type of leading-edge configuration had no effect on the magnitude of the lift increment due to suction in the landing approach ($\alpha=11^\circ$). There was, however, a difference in magnitude at C_{Lmax} which was associated with the type of leading edge used. For the type of leading edge which produced a well-rounded lift-curve top and a satisfactory stall such as the cambered leading edge plus fence, less lift due to suction was realized. This was felt to result from the increased thickness of the boundary layer flowing over the flap at the higher C_L values. This increased boundary-layer thickness was the result of the action of the fence in tending to produce a stall in the area inboard of the fence. The significance of the decrease in lift due to suction at C_{Lmax} compared to that obtained at the approach angle of attack is not definitely known. Evidence is given later, however, that greater reductions in approach speed were realized than the reduction in stalling speed alone.

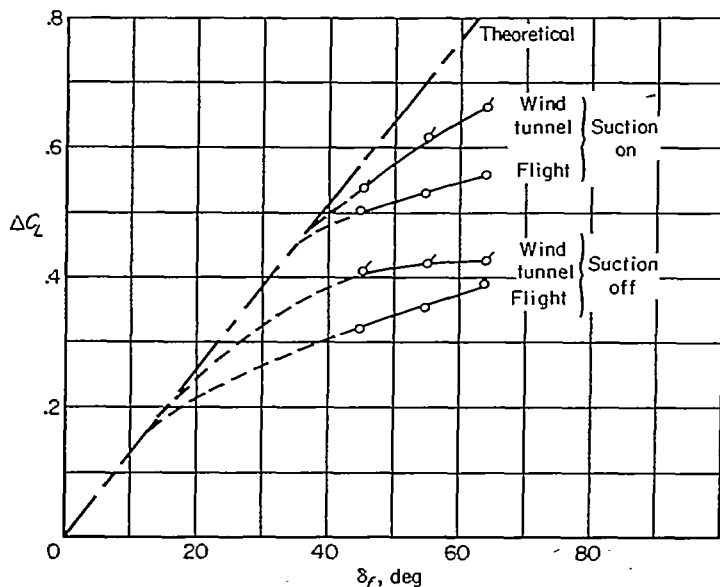


FIGURE 25.—Comparison of flight and wind-tunnel values of flap lift increment with flap deflection angle; $\alpha=6^\circ$.

The variation of flap lift increment with flap deflection is presented in figure 25 for the flight and wind-tunnel tests and compared with theory. The theoretical value was calculated by means of reference 2. The wind-tunnel results have been corrected to the flight airplane flap chord and corrected for trim. The results in figure 25 indicate that the flight flap lift values are less than the tunnel values for both suction on and off. The reason for this is not completely understood. Some of the differences in flap lift are felt to be associated with the effect of the type of wing-fuselage combination used on the flow at the inboard flap edge. In the tunnel tests, a midwing mounting was used in contrast to the low-wing position on the F-86A airplane. A limited

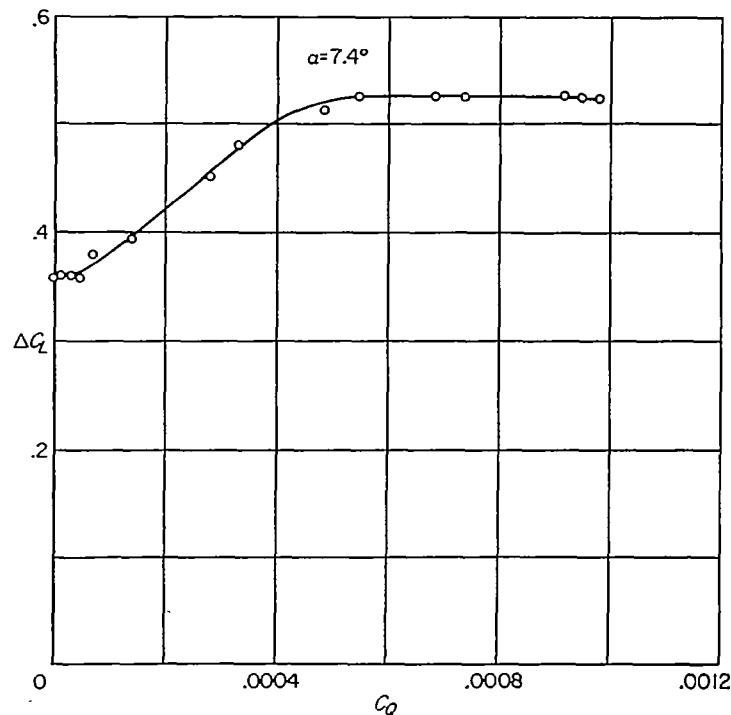


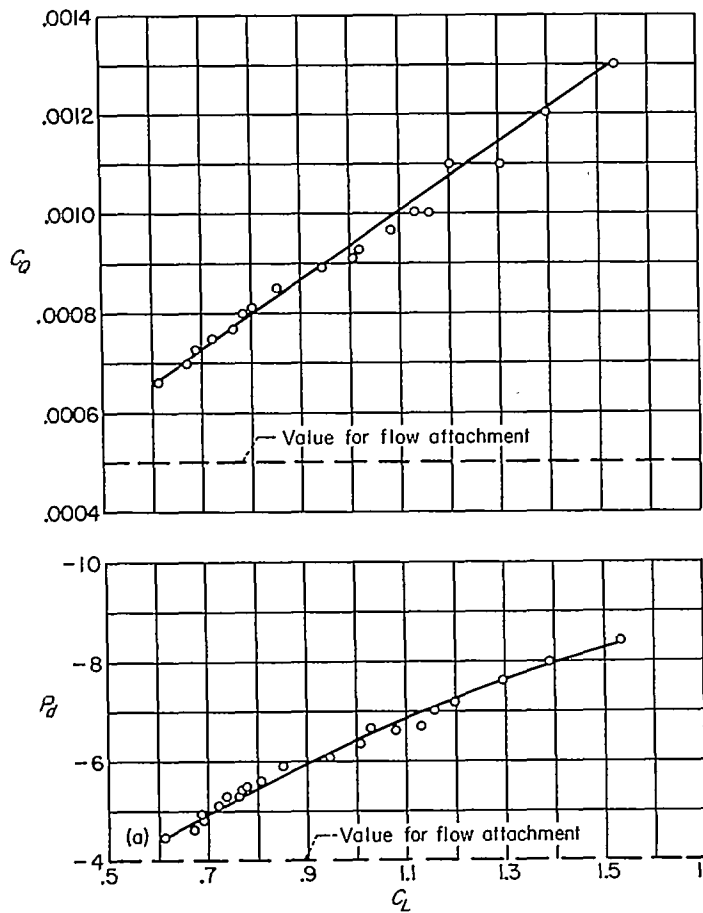
FIGURE 26.—Variation of flap lift increment with flow coefficient; $\delta_f=64^\circ$.

amount of fairing of the upper wing surface of the airplane at the fuselage trailing-edge juncture resulted in improvements in lift due to suction. Other attempts to increase the flap lift, such as a fence on the flap, a seal between the wing and the flap, and turning vanes to direct high energy air over the inboard area of the flap, did little or nothing to improve the lift increment due to suction.

Suction requirements.—Suction requirements are illustrated by the data presented in figure 26 in terms of flap lift increment, ΔC_L , and flow coefficient. These data indicate that the flap lift increased with flow coefficient up to a value of approximately 0.0005, beyond which no further increase in flap lift occurred. These data bear out the results of the wind-tunnel tests regarding the amount of flow coefficient required. A pressure coefficient of -4.0 was necessary to obtain the flow coefficient of 0.0005 at a C_L of 1.0. The values of flow coefficient and pressure coefficient in the flap duct used in the flight tests are shown in figure 27. These data indicate that sufficient flow coefficient and pressure coefficient were used over the speed range of these tests.

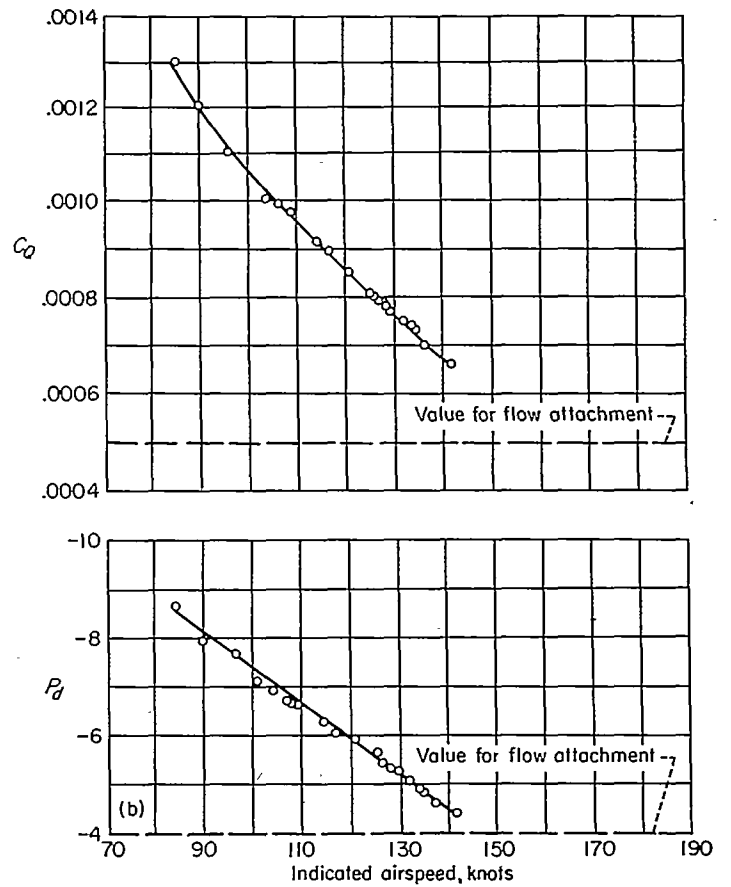
Operational characteristics of boundary-layer control.—One of the main points of interest in the use of boundary-layer control is the effect on the performance and handling characteristics of the airplane. Actual measurements were not made of landing distance, take-off distance, climb, and catapult launchings, but flight measurements of lift, drag, and engine thrust have been used to make computations of the various performance items for a range of gross weights and at standard sea-level conditions. The methods used for computing performance are noted in the appendix.

In evaluation of the landing performance of the airplane with area-suction flaps deflected 55° , the opinions of the 16 pilots, presented in table VI, were used in relating stalling and landing-approach characteristics for the airplane with



(a) Variation C_Q and P_d with C_L .

FIGURE 27.—Pump characteristics obtained over test range with $\delta_f = 64^\circ$.



(b) Variation of C_Q and P_d with velocity.

FIGURE 27.—Concluded.

area-suction flaps as well as for the standard airplane with slotted flaps. The stall data for the two airplane configurations are shown in table VIII, while a compilation of minimum approach speed (or over-the-fence speeds) is shown in table IX. Comparative figures are listed showing the effects of suction alone and of increased flap deflection, as well as comparisons with the standard airplane. Additional data are shown in table X for other configurations of wing leading edge, the slatted leading edge and the cambered leading edge without fence for 55° and 64° deflection of area-suction flap, which were flown by the four research pilots (K, L, M, and N).

The lift coefficient and angle of attack corresponding to each pilot's approach speed are shown on the curves of figure 28 for three configurations of the airplane, with and without suction applied to the plain flaps and with the slotted flaps, and indicate the wide range of angles of attack used by various pilots. The maximum lift coefficient with boundary-layer control shown in this figure is for the configuration evaluated by the 16 pilots. Improvements to the installation later resulted in a slightly higher $C_{L_{max}}$ value, shown in figure 24. Curves of thrust required for level flight plotted against airspeed are presented in figure 29 for the various configurations tested and include the average approach speed chosen by the pilots.

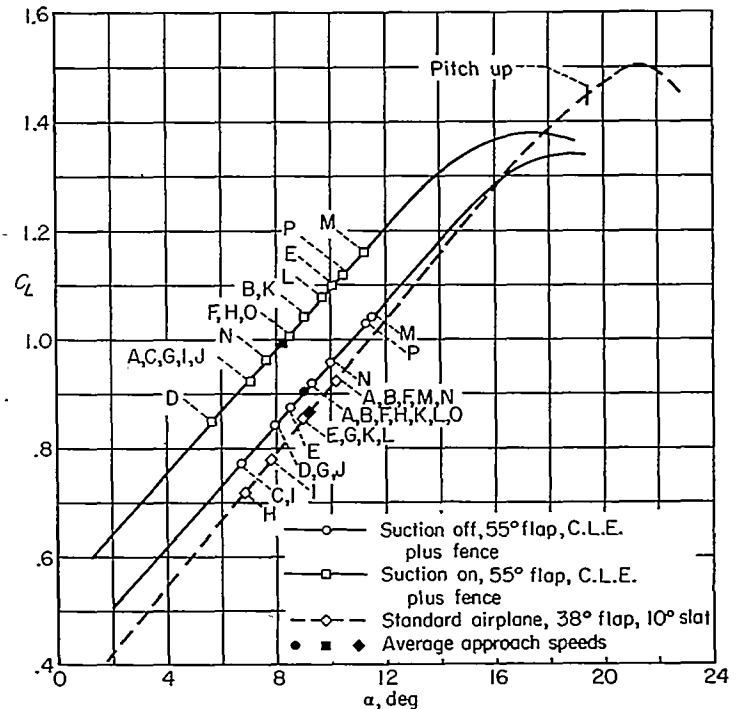


FIGURE 28.—Variation of lift coefficient with angle of attack for the test airplanes with values corresponding to individual pilot's approach speed shown.

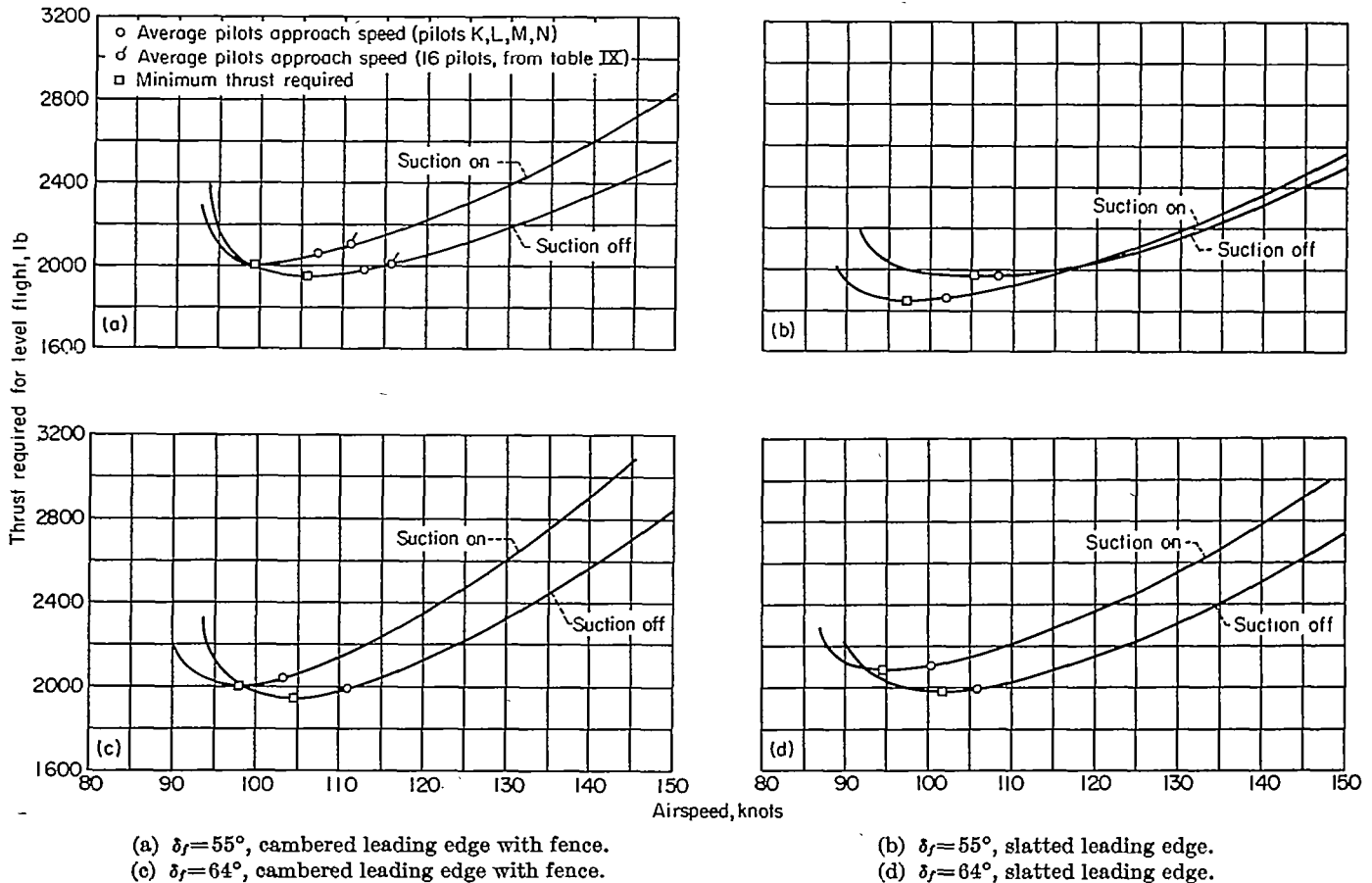


FIGURE 29.—Thrust required for level flight for various configurations of test airplane, gear down and speed brakes out.

There is a wide variety of factors which may be considered by a pilot as affecting his choice of minimum comfortable approach speed. It is possible, and often the case, that several factors are present for one airplane, making selection of a single primary reason difficult because of complex interrelationships. An attempt has been made here, however, to isolate those factors considered of primary importance by the pilots.

Examination of table VI indicates that the pilots' reasons for limiting the approach speed of the various airplanes can be divided into three categories, as follows:

A. Reasons associated with stall characteristics: It would be expected that on airplanes limited by stall characteristics the most direct influence on the approach speed would result from an increase in $C_{L_{max}}$ or improvements in the stalling characteristics.

B. Reasons associated with attitude or visibility limitations: It would be expected that on an airplane limited by this characteristic the most direct influence on approach speed would result from an increase in lift at attitudes below $C_{L_{max}}$.

C. Reasons associated with longitudinal control, that is, ability to control altitude or flight path: A number of factors influence this characteristic. One expected to be of primary importance, which was varied on the test airplanes, was the variation of L/D with α . This variation is evident from the change in the shape of the curve

of thrust required for steady level flight versus speed (fig. 29).

It is of interest to examine the above listed categories in comparison with the approach speed decrements realized from boundary-layer control.

The 16 pilots who flew the airplane with boundary-layer control inoperative gave reasons for limiting approach speed which were almost evenly divided between these categories (table XI).

On the basis of the lift curves presented in figure 28, it would be expected that application of boundary-layer control to the flap would tend to relieve attitude and visibility limitations but would not significantly change stall speed (a ΔV_s of only 1 knot). The pilots' comments are consistent with these changes in that, with boundary-layer control operating, only two considered the attitude or visibility the limiting factor. The average decrease in approach speed was 5.9 knots. Closer examination of this average, however, reveals that the pilots who previously considered Category B or C the limiting factor benefited most from the operation of boundary-layer control to the extent of a 7.9-knot decrease. The pilots who previously had considered proximity to the stall the limiting factor benefited the least to the extent of 3.0 knots. Thus, despite the lack of any dominant limiting factor on this airplane, there is a consistent relationship between the effect of aerodynamic change and the factors which the individual pilot considered limiting on choice of approach speed.

The aerodynamic factors which influence the ease with which the attitude or flight path of the airplane can be controlled are more complex than the Category A and B limitations. However, on all of the configurations tested the average minimum approach speed (fig. 29) lies slightly above the speed for minimum thrust required. For the configurations flown in this investigation, it would appear that the ability to flare or to arrest sink rates deteriorates below the minimum acceptable to the pilot at or near the speed for minimum thrust required and tends to result in his setting his approach speed accordingly. This surmise is not explicitly borne out by the pilots' comments, but it will be observed from table X that the decreases in average approach speed due to boundary-layer control on the flap are related very closely to the corresponding decreases in speed for minimum thrust required. It is noteworthy that the research pilots (K, L, M, and N) who had the most opportunity to fly the test airplanes were consistent in noting Category C (ability to control altitude) as the primary limiting factor establishing the approach speeds on all the configurations with flap boundary-layer control. Category C is also considered as the limiting factor for the standard F-86A-1 by 7 out of the 12 other pilots.

Of the additional configurations flown with flap boundary-layer control (table X), it is of interest to note that the airplane with cambered leading edge and no fence had an unsatisfactory roll-off at the stall but fell in Category C rather than Category A. The airplane with slats and 55° flap deflection, which had excellent stall characteristics, was also limited by Category C and was generally considered the most desirable configuration flown, although it did not result in any appreciable decrease in approach speed over the airplane with cambered leading edge and no fence. A slightly greater decrease in approach speed resulted from increasing the flap deflection to 64°, but the increased drag resulted in less desirable wave-off characteristics.

From the foregoing results, it is apparent that the pilot utilized the increased lift offered by the 64° boundary-layer-control flap to decrease the approach speeds by flying at approximately the same attitude with suction off or on. These speeds correspond to $1.19 V_{stall}$ and $1.15 V_{stall}$ for suction off and on, respectively. Based on these values of approach speed and an assumed touchdown speed of $1.05 V_{stall}$, the effect of boundary-layer control on the landing distance over a 50-foot obstacle was computed and is shown in figure 30 for various gross weights. These data indicate that a 14.5-percent reduction in landing distance due to boundary-layer control would be obtained at 64° flap deflection.

In the computations for take-off and climb, account is taken of the thrust loss incurred as a result of extracting air from the engine compressor. In order to operate the engine within allowable tail-pipe temperature limits with the suction system on, a reduction from 100-percent rpm was necessary for the type of engine tail pipe used in the F-86A airplane. The thrust loss associated with the decreased rpm was approximately 150 pounds. It is assumed that in take-off, the bleed-air valve would be opened only to that amount necessary to reach the C_Q value above which

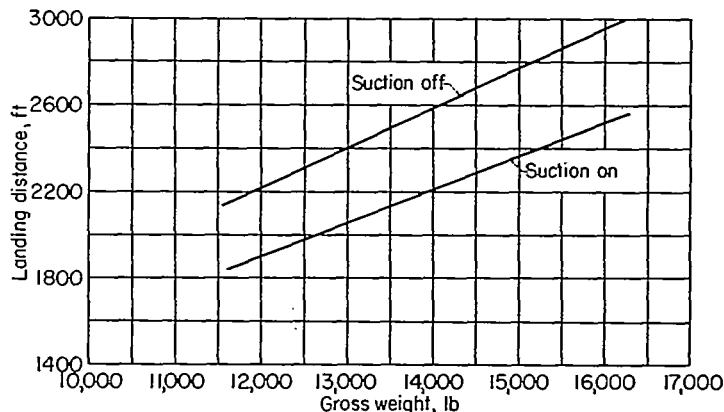


FIGURE 30.—Variation of landing distance over a 50-foot obstacle with gross weight for 64° flap deflection, slatted leading edge, speed brakes out.

no further increase in flap lift occurred (as shown in fig. 26) in order not to penalize unduly the suction system. With a more efficient pumping system (ejector pump used has an efficiency of approximately 15 percent) or a variable exit area type tail pipe, the thrust loss would be reduced appreciably with a resultant gain in performance with suction on.

Consider first catapult take-off. The following assumptions are used in computing the speed at the end of the catapult run. Lift-off speed is selected as the speed at nine-tenths of $C_{L_{max}}$ or at the maximum ground attitude. This speed has the additional restriction that the longitudinal acceleration shall be equal to or greater than $0.065g$.⁵ The results of computations of the take-off speeds at the end of the catapult run as a function of gross weight for various flap deflections with suction on and off are presented in figure 31. Indicated in this figure are the H8 catapult characteristics. The take-off speeds for the 55° and 64° flap-deflection configurations with suction on were based on nine-tenths of $C_{L_{max}}$; the other configurations were limited in take-off speed by ground attitude to the C_L at $\alpha=16^\circ$. At 21,000 pounds or greater, the $0.065g$ acceleration requirement becomes limiting. The data in figure 31 indicate improvements in take-off performance with suction on. By use of the H8 catapult characteristics and the data in figure 31, computations were made of the wind required over the deck as a function of gross weight for the operational pressure limit of 3500 psi, a reduced pressure of 2950 psi, and the catapult end speed limit. These data are presented in figure 32. It can be noted in this figure that when the limit H8 catapult pressure is used, wind is required over the deck only for the very highest gross weights. The data in figure 32 indicate that approximately 6 knots less wind would be required for the flap deflected 64° with suction on, compared with the 38° flap with no suction.

Next, with regard to a field take-off, the assumption is made that the airplane accelerates on the ground in a level attitude, and at take-off speed the airplane is rotated to the angle of attack corresponding to a velocity of $1.2 V_{stall}$. For the transition distance, it is assumed that the airplane

⁵ Assumed minimum acceleration value used to assure that the aircraft does not sink after launch.

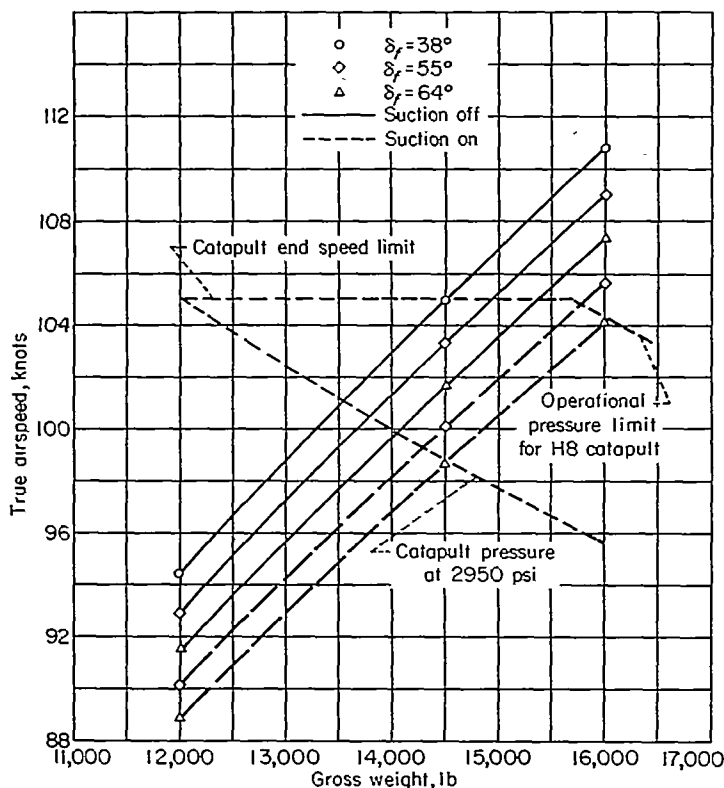


FIGURE 31.—Variation of catapult take-off velocity with gross weight for various flap deflections and boundary-layer control on and off.

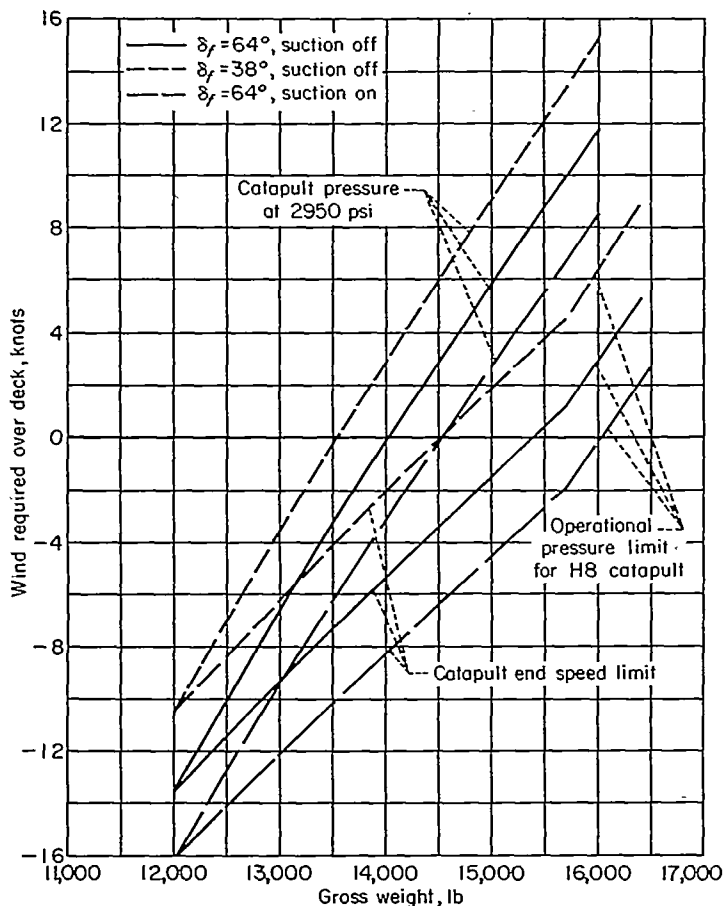


FIGURE 32.—Variation of wind required over deck with gross weight and boundary-layer control on and off.

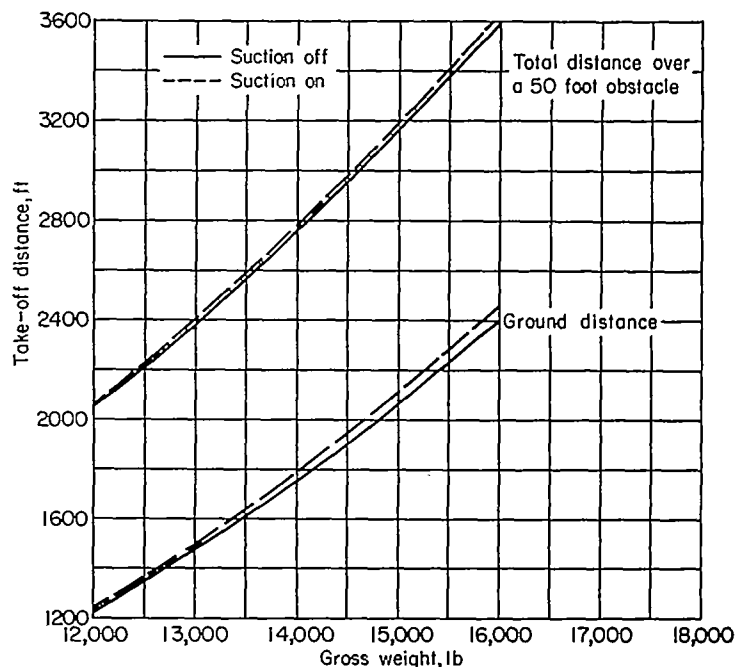


FIGURE 33.—Variation of take-off distance for boundary-layer control on and off; $\delta_f=55^\circ$, slatted leading edge.

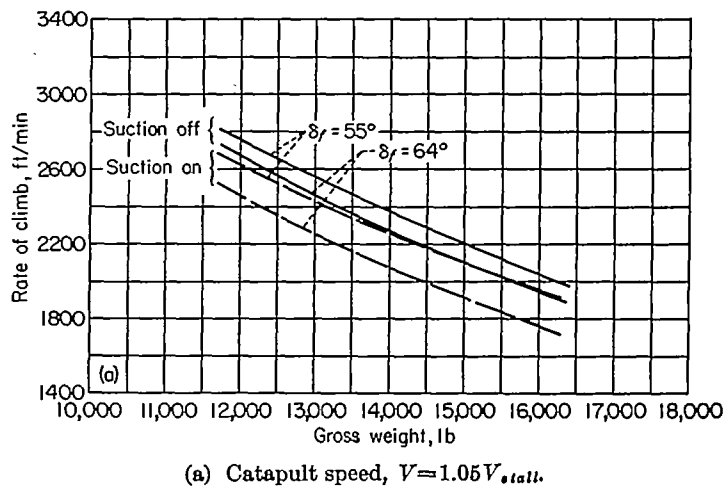


FIGURE 34.—Variation of rate of climb with gross weight for various flap deflections and boundary-layer control on and off; slatted leading edge.

is in a steady rate of climb before attaining the 50-foot-height point. The results of the computations indicate very little change in take-off performance due to boundary-layer control or change in flap deflection. The effect of boundary-layer control on take-off performance is illustrated in figure 33 for 55° flap deflection. For this case, the gains in take-off performance which would result from the use of boundary-layer control are cancelled by the thrust loss associated with the type of pumping system used. The take-off performance could be improved by turning on the boundary-layer control after the airplane has accelerated to the take-off speed.

The rates of climb after a catapult take-off ($1.05 V_{stall}$) and after wave-off ($1.15 V_{stall}$) are presented in figure 34. These data indicate less rate of climb with the boundary-layer control on due to the loss in thrust previously men-

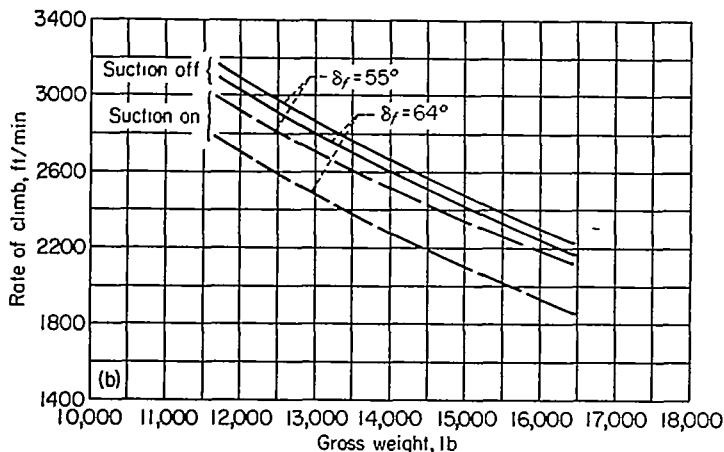

 (b) Wave-off speed, $V = 1.15 V_{stall}$.

FIGURE 34.—Concluded.

tioned. The rate of climb should be adequate, however, over the gross-weight range covered.

Turning the suction off produced a nose-up pitch change which was considered small. No hazardous flight conditions were encountered in simulating loss of suction power at any airspeed. There was no marked change in stick-free stability as a result of the use of boundary-layer control.

Flight tests conducted in areas of moderate rain showed negligible effect of the rain on either the lift due to suction or the pumping requirements. No clogging of the porous material was evident after approximately 50 hours of flight

testing. No particular effort was made to protect the porous area in the hangar. No detrimental effects on engine life due to the use of the air bleed (3 pounds per second, average) were noted for approximately 67 hours of flight testing.

CONCLUDING REMARKS

The results of wind-tunnel and flight tests of a 35° swept-wing airplane having area suction applied to trailing-edge flaps indicated that trailing-edge flap effectiveness could be improved to values approaching theory for flap deflections ranging from 45° to 64° of deflection. The primary effects of boundary-layer control applied to trailing-edge flaps was to increase lift at a given angle of attack. Although the flap boundary-layer control reduced the stall speed only slightly, a reduction in minimum comfortable approach speed of about 12 knots was obtained by a number of pilots, particularly those giving visibility and attitude or longitudinal control as the limiting factor. The improvements in flap effectiveness were accomplished with low values of flow quantity and suction horsepower; flow coefficients ranging from 0.0003 to 0.0008 were required; and suction power ranging from 10 to 25 horsepower would be required in the normal landing-approach and take-off speed ranges.

AMES AERONAUTICAL LABORATORY

NATIONAL ADVISORY COMMITTEE FOR AERONAUTICS

MOFFETT FIELD, CALIF., May 6, 1958

APPENDIX

METHODS USED FOR PERFORMANCE EVALUATION

The following equations and assumptions were used in computing the performance.

Take-off distance:

$$\text{Ground run} = \frac{WV_{T0}^2}{64.4[T - \mu W - Sq(C_D - \mu C_L)]}, \text{ ft}$$

(from ref. 4, pp. 195-196).

$$\text{Air distance} = \frac{50W}{T-D} + \frac{V_{T0}^2}{g\sqrt{2}}, \text{ ft}$$

(ref. 5, p. 51) where take-off velocity

$$\begin{aligned} V_{T0} &= 1.2 V_{stall} \\ &= 1.2 \left(1.71 \sqrt{\frac{W - T \sin \alpha}{C_{Lmax}}} \right), \text{ ft/sec} \end{aligned}$$

and

T = engine thrust

$$q = \frac{\rho}{2} (0.7 V_{T0})^2$$

W = gross weight in pounds

α = angle of attack at C_{Lmax}

$$\mu = 0.02$$

(The assumption is made that steady climb has been reached before the 50-foot height is attained.)

Climb:

$$\text{Rate of climb} = \frac{101.4 VT_{ex}}{W}, \text{ ft/min}$$

where

$$T_{ex} = \text{excess thrust at } V$$

Landing distance:

$$\text{Air distance} = \left[\frac{(V_{50}^2 - V_L^2)}{64.4} + 50 \right] \frac{L}{D}, \text{ ft}$$

$$\text{Ground run} = \frac{V_L^2}{64.4 \left[\mu - \left(\frac{D}{L} \right) \right]} \log_e \left(\frac{L}{D} \right) \mu, \text{ ft}$$

(ref. 6, p. 312) where V_{50} is pilot's actual approach speed, and the landing velocity,

$$V_L = 1.05 V_{stall}$$

and

$$\mu = 0.4$$

Catapult end speed:

$$V_{T0} = \sqrt{\frac{295(W - T \sin \alpha_{T0})}{SC_{LT0}}}, \text{ knots}$$

where

T = thrust at 100-percent rpm

$$C_{LT0} = 0.9 C_{Lmax}$$

$$\alpha_{T0} = \alpha \text{ at } C_{LT}$$

REFERENCES

1. Holzhauser, Curt A., and Bray, Richard S.: Wind-Tunnel and Flight Investigations of the Use of Leading-Edge Area Suction for the Purpose of Increasing the Maximum Lift Coefficient of a 35° Swept Wing Airplane. NACA Rep. 1276, 1956. (Supersedes NACA RM A52G17 and RM A55C07)
2. DeYoung, John: Theoretical Symmetric Span Loading Due to Flap Deflection for Wings of Arbitrary Plan Form at Subsonic Speeds. NACA Rep. 1071, 1952.
3. Anderson, Seth B., Matteson, Frederick H., and Van Dyke, Rudolph D., Jr.: A Flight Investigation of the Effect of Leading-Edge Camber on the Aerodynamic Characteristics of a Swept-Wing Airplane. NACA RM A52L16a, 1953.
4. Perkins, Courtland D., and Hage, Robert E.: Airplane Performance Stability and Control. John Wiley & Sons, Inc., 1949.
5. Lush, Kenneth J.: Standardization of Take-Off Performance Measurements for Airplanes. Tech. Note R-12, USAF, ARDC, Air Force Flight Test Center, Edwards, Calif., 1954.
6. Dwinell, James H.: Principles of Aerodynamics. McGraw-Hill Book Co., Inc., 1949.

TABLE I.—DIMENSIONS OF MODEL AND TEST AIRPLANE

Wing	
Total area, sq ft.....	287.9
Span, ft.....	37.12
Aspect ratio.....	4.79
Taper ratio.....	0.51
Mean aerodynamic chord (wing station 98.7 in.), ft.	8.1
Dihedral angle, deg.....	3.0
Sweepback of 0.25-chord line.....	35°14'
Geometric twist, deg.....	2.0
Root airfoil section (normal to 0.25-chord line)	NACA 0012-64 modified
Tip airfoil section (normal to 0.25-chord line)	NACA 0011-64 modified
Wing area affected by flaps, sq ft.....	116.6
Flap	
Wind-tunnel model	
Flap area (total), sq ft.....	29.8
Flap span (from 13.5 to 49.5-percent semispan), ft.....	7.27
Flap chord (constant), ft.....	2.108
Test Airplane	
Flap area (total), sq ft.....	23.7
Flap span (from 13.5 to 49.5-percent semi- span), ft.....	7.27
Flap chord (constant), ft.....	1.67

TABLE II.—COORDINATES OF THE WING AIRFOIL SECTIONS NORMAL TO THE WING QUARTER-CHORD LINE AT TWO SPAN STATIONS

[Dimensions given in inches]

Section at 0.467 semispan			Section at 0.857 semispan		
x	z		x	z	
	Upper surface	Lower surface		Upper surface	Lower surface
0	0.231	-----	0	-0.098	-----
.119	.738	-0.307	.089	.278	-0.464
.239	.943	-.516	.177	.420	-.605
.398	1.127	-.698	.295	.562	-.739
.597	1.320	-.895	.443	.701	-.879
.996	1.607	-1.196	.738	.908	-1.089
1.992	2.104	-1.703	1.476	1.273	-1.437
3.984	2.715	-2.358	2.952	1.730	-1.878
5.976	3.121	-2.811	4.428	2.046	-2.176
7.968	3.428	-3.161	5.903	2.290	-2.401
11.952	3.863	-3.687	8.855	2.648	-2.722
15.936	4.157	-4.064	11.806	2.911	-2.944
19.920	4.357	-4.364	14.758	3.104	-3.102
23.904	4.480	-4.573	17.710	3.244	-3.200
27.888	4.533	-4.719	20.661	3.333	-3.250
31.872	4.525	-4.800	23.613	3.380	-3.256
35.856	4.444	-4.812	26.564	3.373	-3.213
39.840	4.299	-4.758	29.516	3.322	-3.126
43.825	4.081	-4.638	32.467	3.219	-2.989
47.809	3.808	-4.452	35.419	3.074	-2.803
51.793	3.470	-4.202	38.370	2.885	-2.574
55.777	3.066	-3.891	41.322	2.650	-2.302
59.761	2.603	-3.521	44.273	2.374	-1.986
63.745	2.079	-3.089	47.225	2.054	-1.625
83.681	-.740	-----	63.031	.321	-----
L. E. radius: 1.202, center at 1.201, 0.216			L. E. radius: 0.822, center at 0.822, -0.093		

* Straight lines to trailing edge.

TABLE III.—SUMMARY OF EXTENT AND POSITIONS OF POROUS SURFACE TESTED ON SUCTION FLAP; DIMENSIONS NORMAL TO HINGE REFERENCE LINE

[Dimensions in inches]

Configuration no.	Extent of chordwise opening	Position of forward edge (aft of ref. line)	Flap deflection, deg	Configuration no.	Extent of chordwise opening	Position of forward edge (aft of ref. line)	Flap deflection, deg
1	2.5	2.5	45, 55	20	3.0	1.0	64
2	2.5	3.5	45, 55, 64	21	3.0	2.0	64
3	2.5	1.5	45	22	3.0	3.0	64
4	2.5	4.5	55	23	3.0	4.0	64
5	2.5	4.5	55	24	4.0	2.0	64
6	.5	2.5	55	25	4.5	1.5	64
7	1.0	2.5	55	26	5.0	2.0	64
8	1.5	2.5	55	27	1.25	1.87	70
9	3.5	2.5	55	28	2.62	1.87	70
10	5.5	2.5	55	29	3.12	1.87	70
11	1.5	.5	55	30	3.62	1.87	70
12	1.5	1.5	55	31	4.12	1.87	70
13	1.5	3.5	55	32	5.12	1.87	70
14	1.5	4.5	55	33	3.62	2.12	70
15	1.5	5.5	55	34	3.62	2.32	70
16	1.5	6.5	55	35	3.62	2.62	70
17	1.0	2.0	64	36	3.62	3.12	70
18	2.0	2.0	64	37	3.62	3.62	70
19	2.0	2.5	64	38	3.62	4.12	70

TABLE IV.—COORDINATES OF THE MODIFIED WING LEADING EDGE AT TWO SPAN STATIONS, NORMAL TO THE WING QUARTER-CHORD LINE

[Dimensions given in inches]

Section at 0.467 semispan			Section at 0.857 semispan		
x	z		x	z	
	Upper surface	Lower surface		Upper surface	Lower surface
-1.692	-1.445	-----	-1.250	-1.359	-----
-1.273	-.348	-2.552	-.934	-.495	-2.192
-.855	.222	-2.898	-.619	-.099	-2.454
-.436	.629	-3.114	-.304	.197	-2.609
-.018	.969	-3.272	.011	.456	-2.701
.400	1.266	-3.391	.326	.675	-2.769
.819	1.527	-3.473	.641	.867	-2.796
1.237	1.760	-3.523	.956	1.040	-2.813
1.655	1.952	-3.549	1.272	1.189	-2.821
1.992	2.104	-----	1.476	1.273	-----
2.074	-----	-3.552	1.587	-----	-2.813
2.911	-----	-3.531	2.217	-----	-2.787
4.166	-----	-3.481	3.163	-----	-2.742
6.258	-----	-3.472	4.739	-----	-2.709
8.350	-----	-3.542	6.314	-----	-2.712
10.442	-----	-3.657	7.890	-----	-2.751
14.626	-----	-3.956	9.466	-----	-2.808
15.936	-----	-4.064	11.042	-----	-2.885
			11.806	-----	-2.944
L. E. radius: 1.674, center at -0.018, -1.445			L. E. radius: 1.261, center at 0.011, -1.359		

TABLE V.—LOCATION OF SURFACE PRESSURE ORIFICES

[Position of orifices,¹ chordwise percent]

Orifice No.	0.25 <i>b</i> /2 and 0.45 <i>b</i> /2 station		0.65 <i>b</i> /2 and 0.85 <i>b</i> /2 station	
	Upper surface	Lower surface	Upper surface	Lower surface
1	0	-----	0	-----
2	. 25	0. 25	. 25	0. 25
3	. 5	. 5	. 5	. 15
4	1. 0	1. 0	1. 0	1. 0
5	1. 5	1. 5	1. 5	1. 5
6	2. 0	2. 0	2. 0	2. 0
7	2. 5	2. 5	2. 5	2. 5
8	3. 5	3. 5	3. 5	3. 5
9	5. 0	5. 0	5. 0	5. 0
10	7. 5	7. 5	7. 5	7. 5
11	10. 0	10. 0	10. 0	10. 0
12	15. 0	15. 0	15. 0	15. 0
13	20. 0	20. 0	20. 0	20. 0
14	30. 0	30. 0	30. 0	30. 0
15	40. 0	40. 0	40. 0	40. 0
16	50. 0	70. 0	50. 0	60. 0
17	60. 0	75. 0	60. 0	70. 0
18	70. 0	80. 0	70. 0	80. 0
19	75. 0	88. 0	80. 0	90. 0
20	80. 0	90. 5	90. 0	97. 5
21	83. 3	93. 2	97. 5	-----
22	84. 0	96. 0	-----	-----
23	84. 4	98. 0	-----	-----
24	84. 8	-----	-----	-----
25	85. 4	-----	-----	-----
26	86. 5	-----	-----	-----
27	87. 7	-----	-----	-----
28	91. 0	-----	-----	-----
29	93. 0	-----	-----	-----
30	95. 0	-----	-----	-----
31	97. 0	-----	-----	-----
32	99. 0	-----	-----	-----

¹ Upper surface orifices omitted:
 Station 0.25*b*/2, no. 6.
 Station 0.85*b*/2, nos. 2, 6,
 and 11.
 Station 0.65*b*/2, no. 7.

Lower surface orifices omitted:
 Station 0.25*b*/2, no. 16.
 Station 0.65*b*/2, nos. 6, 7,
 and 8.
 Station 0.85*t*/2, no. 10 above
 12.8.

TABLE VI.—PILOTS' COMMENTS RELATING TO STALL AND APPROACH CHARACTERISTICS

(a) Configuration I: Standard F-86A-1; 38° flap; slats

Pilot	Suction B. L. C.	Stall speed, I. A. S., knots	Stall characteristics	Approach speed I. A. S., knots	Primary reasons for choosing approach speed
A	-----	98-100	Warning: Lightening of stick forces. Stall: Satisfactory. Mild pitch-up and roll-off.	115-----	Visibility is limiting factor. Have good control down to 105, but attitude best at 115-120. At about 100 much larger stick movement is necessary for control. Approach speed dependent upon gustiness.
B	-----	98	Warning: Marginally satisfactory. Force lightening at 105-102 and pitch-up at 102. No aerodynamic warning. Stall: Satisfactory. Mild buffet, left roll-off, easy to control. Ailerons more effective than elevator at stall.	115-----	115 chosen to give adequate speed above stall (in this case 105 where force lightening occurred). L. S. O. (Landing Signal Officer) would add 15 to stall for approach speed. Pilot chooses a minimum of 10. Airplane flyable at any speed above stall. Elevator control good at 110. At 110-115 visibility is a problem but would not be if seat could be raised. Considerable floating experienced at 115.
E	-----	102	Warning: None. Stall: Slight pitch-up, left wing drop, incipient spin.	130 on final. 120 over fence.	Forward visibility.
F	-----	97-101	Warning: Insufficient. Stall: Satisfactory. Moderate pitch-up and roll-off.	115-----	Poor lateral control and normal margin for flare out. Better lateral control and feel on suction flap airplane. Worse sink rate than suction flap airplane suction on.
G	-----	99	Warning: Light buffet 110. Yaws left at 103 but controllable. Stall: Very good. Slow left wing drop.	130 on final. 120 over fence 110 touchdown.	Pattern felt comfortable by touching down at 110 with no buffet or yaw.
H	-----	100	Warning: Good. Light buffet and pitch-up at 105. Stall: No comments.	130-----	Limited by visibility and feel of aircraft. Lack of adequate seat adjustment restricts visibility over nose more than on suction-flap airplane. Less able to rack around at 120 than suction-flap airplane.
I	-----	100	Warning: Good. 3-6 above stall. Stall: Good to excellent.	125 over fence. 115-110 on touchdown.	Comfortable attitude, visibility. Not worried about hitting tailpipe.
K	-----	100	Stall: Satisfactory.	120-----	Decrease in ability to control altitude by longitudinal control alone.
L	-----	100	Stall: Satisfactory. Mild pitch-up and roll-off.	120-----	Loss of longitudinal control. No stick centering from trim at approach speed.
M	-----	101-102	Stall: Unsatisfactory. Due to pitch-up.	115-----	Positive altitude control.
N	-----	101	Warning: Unsatisfactory. Very little. Stall: Satisfactory.	115-----	No comment.

TABLE VI.—PILOTS' COMMENTS RELATING TO STALL AND APPROACH CHARACTERISTICS—Continued

(b) Configuration II: F-86A-5; 55° suction flap; C. L. E. plus fence

Pilot	Suction B. L. C.	Stall speed, I. A. S., knots	Stall characteristics	Approach speed I. A. S., knots	Primary reasons for choosing approach speed
A	Off	100	Warning: Weak buffet. Stall: Very satisfactory. Mild pitching, very gentle.	115-----	Proximity to stall. Good control 100 up. Good visibility 115-118. No notice- able difference between suction on and off.
	On	100		115-----	
B	Off	100	Warning: Too close but adequate. Stall: Mild, satisfactory.	115-----	Limited by visibility at 110. Control is satisfactory right down to stall. Longitudinal control too sensitive at approach speeds. More positive stick-free stability as on F-86F is more desirable.
	On	95-98	Warning: Too close but adequate. Stall: Mild, satisfactory.	108-----	Limited by nearness to stall. Visibility was not limiting at 110. Attitude is more desirable with suction on, but without lower stall speed, would not lower approach speed.
C	Off	100	Stall: Satisfactory.	125-----	Minimum positive control for gusts or emergency.
	On	95	Stall: Good.	115-----	Has better control and stability than with suction off. No visibility prob- lem.
D	Off	100	Warning: Buffeting, slight wing roll. Stall: Satisfactory.	140 base. 120 over fence. 110 touchdown.	Adequate speed above stall. Feels com- fortable at 110. Satisfactory stall allows coming to within 10 of stall.
	On	99	Warning: Buffeting and slight wing, roll. Stall: Satisfactory.	140 base. 120 over fence. 105 touchdown.	Adequate speed above stall. Decreased attitude allows lower touchdown speed. Visibility not a problem at base and final approach speeds used but noticeably improved on touch- down.
E	Off	98	Warning: High angle of attack, shaking and wallowing of airplane at 102 (more than suction on). Stall: Satisfactory, nose drops through.	125-130 on final. 115-120 over fences.	Optimum visibility with more than ade- quate airspeed. No control diffi- culties.
	On	97	Warning: None. Stall: Satisfactory. Consists of wing drop which is controllable but worse than suction off. Inconsistent: wing drops or stalls straight ahead.	115 on final. 105 over fence.	Decrease in approach speed due to better visibility. Not limited other- wise. Possibly could use 110 ap- proach speed on final. Over fence speed limited by fear of dragging tail.
F	Off	92-97	Warning: Good (100-103). Stall: Satisfactory. Pitch-up followed by pitch-down.	115-----	Limited by concern about ability to flare and the time spent in transition- power off.
	On	90-94	Warning: Inadequate. Stall: Satisfactory.	110-----	Limited by lack of stall warning. Like increased visibility with suction. Suction also reduces rate of sink. Flared better than anticipated but may have been influenced by carrying more power than usual. Flies better 5-10 above stall than suction off.
G	Off	101	Warning: O. K. Bumble at 115, slight left yaw at 102. Stall: Satisfactory. Slight left roll tend- ency.	130 on final. 120 over fence. 110 touchdown.	Limited by speed above yaw and stall. Sink rate higher than suction on.

TABLE VI.—PILOTS' COMMENTS RELATING TO STALL AND APPROACH CHARACTERISTICS—Continued

(b) Configuration II; F-86A-5; 55° suction flap; C. L. E. plus fence

Pilot	Suction B. L. C.	Stall speed, I. A. S., knots	Stall characteristics	Approach speed I. A. S., knots	Primary reasons for choosing approach speed
G	On	99	Warning: Satisfactory. Light buffet at 105. Stall: Satisfactory. Straight ahead.	120 on final. 115 over fence. 105 touchdown.	Limited by speed above stall. Speed on base and final very comfortable 120 kts. due to increased ability to turn. Feels better suction on, especially in jet wash (i. e., turbulence). Could tighten pattern suction on. Decrease in attitude very significant, may influence reduction in approach speed.
H	Off	99	Warning: Satisfactory. Light buffet. Stall: Satisfactory.	115-----	Limited by proximity to stall. Added flap deflection 55° over 38° quite apparent, gave large improvement, more than that due to effect of suction.
	On	94-97	Warning: Light to moderate buffet; more than suction off. Stall: Satisfactory.	110-----	Limited by general feel in approach. Decrease in sink rate with suction on. A more solid feel, especially in turns. Decrease in attitude quite noticeable. Not limited by nearness to stall.
I	Off	100-101	Warning: Good. Buffet 3 less than normal F-86.	125 (power on approach).	Comfortable attitude. Not worried about proximity to stall.
	On	98	Warning: Good. Buffet 3 less than normal F-86.	115 over fence 110 touchdown.	Speed above stall. Attitude improved. Maneuvering in approach felt better.
J	Off	100	Warning: Wing drop and buffet 2 or 3 above stall.	120-----	Attitude. Sufficient speed above stall.
	On	97	Warning: Sufficient. Right wing drop and buffet. 2 or 3 above stall.	115-----	Feels comfortable. Proximity to stall. With more power on would be comfortable at 110.
K	Off	95	Stall: Satisfactory.	115-----	Decrease in ability to control altitude by longitudinal control alone. Visibility.
	On	90	Stall: Satisfactory.	108-----	Decrease in ability to control altitude by longitudinal control alone. Visibility improved over suction off but becomes contributing factor again at this lower speed.
L	Off	95	Warning: Satisfactory. Buffet 3-4 before stall. Stall: Satisfactory. Mild pitch-up, straight ahead.	115-----	Loss of longitudinal control or ability to adequately control altitude.
	On	90	Warning: Marginal. Buffet 2-3 before stall. Stall: Satisfactory. Mild pitch-up, straight ahead.	105-107-----	Loss of longitudinal control or ability to adequately control altitude.
M	Off	95-97	Warning: Marginal. Buffet 98. Stall: Satisfactory.	105-110-----	Ability to stop sink rate.
	On	92-95	Warning: Marginal. Buffet 98. Stall: Satisfactory.	100-105-----	Ability to stop sink rate.
N	Off	98	Warning: Marginal. Buffet at 106. Stall: Good.	110-115-----	Adequate margin above stall.
	On	98	Warning: Marginal. Buffet at 106. Stall: Good.	110-115-----	Adequate margin above stall. Visibility good suction on. Pilot noted no difference in approach speed suction on or off but did note improved visibility.

TABLE VI.—PILOTS' COMMENTS RELATING TO STALL AND APPROACH CHARACTERISTICS—Concluded

(b) Configuration II; F-86A-5; 55 suction flap; C. L. E. plus fence

Pilot	Suction B. L. C.	Stall speed, I. A. S., knots	Stall characteristics	Approach speed I. A. S., knots	Primary reasons for choosing approach speed
O	Off	98	Warning: Mild aileron buffet 102. Stall: Good except for mild pitch-up.	120 on base. 115 over fence. 100 touchdown.	Ability to pull g.
	On	92	Warning: Mild aileron buffet 96. Stall: Good except for mild pitch-up.	110 on base. 110 over fence. 95 touchdown.	Ability to pull g.
P	Off	100	Satisfactory.	108-----	Proximity to stall.
	On	99	Satisfactory.	104-----	Proximity to stall.

TABLE VII.—SUCTION FLOW COEFFICIENT, PRESSURE COEFFICIENT, AND HORSEPOWER REQUIREMENTS

(a) Porous surfaces having low-pressure-drop characteristics

<i>W/S</i> , 40 lb/sq ft										
Flap deflection, 55°						Flap deflection, 64°				
α deg	C_L	V , ft/sec	C_{q_f}	P_{r_f}	Measured suction, hp	C_L	V , ft/sec	C_{q_f}	P_{r_f}	Measured suction, hp
0.5	0.79	206	0.00047	-4.4	23.0	0.92	191	0.00078	-6.8	44.0
4.6	1.06	178	.00050	-4.2	15.7	-----	-----	-----	-----	-----
6.6	-----	-----	-----	-----	-----	1.30	160	.00082	-6.3	24.6
10.9	1.45	152.5	.00062	-3.5	10.1	1.52	148	.00082	-6.0	18.1
15.1	1.68	141.5	.00065	-3.0	6.7	-----	-----	-----	-----	-----
<i>W/S</i> , 60 lb/sq ft										
0.6	0.78	255	0.00049	-4.5	43.7	0.92	237	0.00079	-6.9	87.5
4.6	1.04	220	.00052	-4.2	28.5	-----	-----	-----	-----	-----
6.6	-----	-----	-----	-----	-----	1.29	209	.00082	-6.4	56.0
10.9	1.44	187.6	.00056	-3.8	16.9	1.51	187	.00080	-6.0	33.8
13.0	1.6	179.5	.00058	-3.4	14.0	-----	-----	-----	-----	-----

TABLE VII.—SUCTION FLOW COEFFICIENT, PRESSURE COEFFICIENT AND HORSEPOWER REQUIREMENTS—Concluded

(b) Porous surface having variable- and high-pressure-drop characteristics

<i>W/S</i> , 40 lb/sq ft										
¹ Flap deflection, 55°						² Flap deflection, 64°				
α deg	C_L	V , ft/sec	C_{q_f}	P_{r_f}	Measured suction, hp	C_L	V , ft/sec	C_{q_f}	P_{r_f}	Measured suction, hp
0.5	0.83	202	0.00022	-5.3	12.5	0.92	191	0.00054	-6.8	28.0
6.6	-----	-----	-----	-----	-----	1.28	162	.00050	-6.3	15.8
10.9	1.46	151.5	.00035	-4.8	8.3	1.52	148.5	.00050	-6.0	12.4

¹ $\delta f = 55^\circ$, variable-pressure-drop tapered-thickness porous material.

² $\delta f = 64^\circ$, high-pressure-drop constant-thickness porous material.

TABLE VIII.—STALL DATA—LANDING APPROACH CONFIGURATION

Pilot	I. Standard F-86A-1; 38° flap; slats			II. F-86A-5; 55° suction flap; C. L. E. plus fence					
	V_{stall} knots ¹	Opinion of warning	Opinion of stall	Suction off			Suction on		
				V_{stall} knots ¹	Opinion of warning	Opinion of stall	V_{stall} knots ¹	Opinion of warning	Opinion of stall
A.....	91-95	Satisfactory...	Satisfactory...	99	Weak.....	Satisfactory...	99	Weak.....	Satisfactory.
B.....	91	Marginal.....	Satisfactory...	99	Adequate.....	Satisfactory...	93-96	Adequate.....	Satisfactory.
C.....	---	-----	-----	99	-----	Satisfactory...	92	-----	Good.
D.....	---	-----	-----	99	-----	Satisfactory...	98	-----	Satisfactory.
E.....	97	No warning...	-----	96	-----	Satisfactory...	95	None.....	Satisfactory.
F.....	90-96	Insufficient...	Satisfactory...	89-95	Good.....	Satisfactory...	87-91	Inadequate...	Satisfactory.
G.....	93	-----	Good.....	100	Satisfactory...	Satisfactory...	98	Satisfactory...	Satisfactory.
H.....	95	Good.....	-----	97	Satisfactory...	Satisfactory...	91-95	-----	Satisfactory.
I.....	95	Good.....	Good.....	99-100	Good.....	-----	96	Good.....	-----
J.....	---	-----	-----	99	-----	-----	95	Adequate.....	-----
K.....	95	-----	Satisfactory...	94	-----	Satisfactory...	90	-----	Satisfactory.
L.....	95	-----	Satisfactory...	94	Satisfactory...	Satisfactory...	90	Marginal.....	Satisfactory.
M.....	96-97	-----	Unsatisfactory...	93-95	Marginal.....	Satisfactory...	89-93	Marginal.....	Satisfactory.
N.....	96	Unsatisfactory...	Satisfactory...	97	Marginal.....	Good.....	97	Marginal.....	Good.
O.....	---	-----	-----	96	-----	Good.....	89	-----	Good.
P.....	---	-----	-----	99	-----	Satisfactory...	97	-----	Satisfactory.
Average pilot's calibrated stall speed.	94.6	Unsatisfactory to good.	Satisfactory to good.	97.1	Marginal to satisfac- tory.	Satisfactory...	94.0	Marginal.....	Satisfactory to good.
Measured stall speed $V_{C_{L_{max}}}$ for (W/S) _A	88.5	-----	-----	93.9	-----	-----	92.9	-----	-----

¹ Extrapolation of the airspeed calibration curves of figure 9 has been required for some of these values.

TABLE IX.—APPROACH SPEEDS OR OVER-THE-FENCE SPEEDS CHOSEN

Configuration	Suction	Calibrated approach speed in knots for each pilot																Average
		A	B	C	D	E	F	G	H	I	J	K	L	M	N	O	P	
I. Standard F-86A-1; 38° flap; slats.	-----	114	114	---	---	118	114	118	130	125	---	118	118	114	114	---	---	117.9
II. F-86A-5; 55° suction flap; C. L. E. plus fence.	Off.---	115	115	126	121	115 121	115	121	115	126	121	115	115	105 110	110 115	115	108	116.0
	On.---	115	108	115	121	105	110	115	110	115	115	108	105 107	99 105	110 115	110	104	110.8
Decrease in approach speed due to added flap deflection.	-----	-1	-1	---	---	+3 -2	-1	-2	15	-1	---	3	3	4 9	+4 -1	---	---	2.1
Decrease in approach speed due to addition of flap BLC.	-----	0	7	11	0	10 16	5	6	5	11	6	7	8 10	5	0	5	4	5.9

TABLE X.—COMPILATION OF CALIBRATED LANDING-APPROACH AIRSPEED DATA ON ALL CONFIGURATIONS FOR THE PILOTS FLYING THE COMPLETE EVALUATIONS

Pilot	Configuration I. Standard airplane	Configuration II. 55° flap; C. L. E. plus fence		Configuration III. 55° flap; C. L. E. no fence		Configuration IV. 55° flap; slats		Configuration V. 64° flap; C. L. E. and fence		Configuration VI. 64° flap; slats	
		Suction		Suction		Suction		Suction		Suction	
		Off	On	Off	On	Off	On	Off	On	Off	On
K.....	118	115	108	110	101-105	110	101-105	110	102	105	100
L.....	118	115	105-107	115	108	112	105	115	107	-----	-----
M.....	114	105-110	99-105	105	99	105	95-100	110-112	99-105	105-110	100
N.....	114	110-115	110-115	110-115	105	107-108	102-105	108-110	102	105	100-102
Average pilot's calibrated approach speed, knots.....	116.0	112.5	107.1	110.6	103.7	108.6	102.2	111.2	103.2	105.8	100.3
Average decrease in approach speed due to added flap deflection, knots....	-----	3.5		5.4		7.4		4.8		9.5	
Average decrease in approach speed due to addition of suction BLC, knots....	-----	5.4		6.9		6.0		8.0		5.5	
Average decrease in approach speed below standard airplane, knots.....	-----	8.9		12.3		13.4		12.8		15.0	
Measured stall speed $V_{C_{L_{max}}}$ for $(W/S)_A$, knots....	88.5	93.9	92.9	85.3	82.1	90.2	88.4	91.7	89.4	89.3	87.3
Ratio of average approach speed to measured stall speed, knots.....	1.31	1.20	1.15	1.30	1.26	1.20	1.16	1.21	1.16	1.19	1.15
Decrease in speed for minimum thrust required due to suction BLC, knots.....	-----	6.3		-----		8.0		6.7		7.0	

TABLE XI.—PRIMARY REASONS FOR LIMITING APPROACH SPEEDS

Category	Reasons	I. Standard F-86A-1; 38° flap; slats	II. F-86A-5; 55° suction flap; C. L. E. plus fence		III-VII. F-86A; suction flap (all configurations)
			Suction off	Suction on	Suction on or off
A	Proximity to stall.....	B.....	A, D, G, H, J, N, P.	A, B, D, G, I, J, N, P.	
	Proximity to yaw.....				
	Poor stall characteristics.....			F.....	
	Number of pilots limiting because of stall characteristics.	1.....	7.....	8.....	
B	Visibility.....	A, B, E, H, I...	B, E, L.....	E, L.....	
	Attitude.....	A, I.....	I, J.....		
	Concern for dragging tail.....			E.....	
	Number of pilots limiting because of attitude or visibility characteristics.	5.....	5.....	2.....	
C	Minimum positive longitudinal or altitude control.....	F, K, L, M, N..	C, K, L.....	C, K, L.....	K, L, M, N.
	Ability to flare, maneuver or arrest sink.....	F.....	F, M, O.....	M, O.....	K, L, M, N.
	Feel.....	G, H.....		H.....	
	Number of pilots limiting for altitude or longitudinal control characteristics.	7.....	6.....	6.....	4.

